HHS Public Access

Author manuscript

Immunity. Author manuscript; available in PMC 2017 June 21.

Published in final edited form as:

Immunity. 2016 June 21; 44(6): 1299–1311. doi:10.1016/j.immuni.2016.02.018.

Fine-tuning of CD8 T cell mitochondrial respiration by MCJ/DnaJC15 dictates protection to influenza virus

Devin P. Champagne[1], **Ketki M. Hatle**[1], **Karen A. Fortner**[1], **Angelo D'Alessandro**[2], **Tina M. Thornton**[1], **Rui Yang**[1], **Daniel Torralba**[1], **Julen Tomás-Cortázar**[3], **Yong Woong Jun**[4], **Kyo Han Ahn**[4], **Kirk C. Hansen**[2], **Laura Haynes**[5], **Juan Anguita**[3,6], and **Mercedes Rincon**[1,*]

[1]Program in Immunobiology, Department of Medicine, University of Vermont, Burlington, Vermont, 05405 USA

[2]Department of Biochemistry and Molecular Genetics, University of Colorado Denver, Aurora, CO 80045, USA

[3]Center for Cooperative Research in Biosciences (CIC bioGUNE), Derio 48160 Bizkaia, Spain

[4]Department of Chemistry, Center for Electro-Photo Behaviors in Advanced Molecular Systems, Pohang University of Science and Technology (POSTECH), Nam-Gu, Pohang, 790-784 Gyeongbuk, Republic of Korea

[5]Center on Aging and Department of Immunology, University of Connecticut Health Center, Farmington, CT 06030 USA

[6]Ikerbasque, Basque Foundation for Science, Bilbao, Bizkaia, Spain

SUMMARY

Mitochondrial respiration is tightly regulated in CD8 T cells during the transition from naïve to effector and memory cells, but the mechanisms that control this process have not been defined. Here we show that MCJ/DnaJC15 acts as an endogenous break for mitochondrial respiration in CD8 T cells by interfering with the formation of electron transport chain (ETC) respiratory supercomplexes. Metabolic profiling reveals an enhanced mitochondrial metabolism in MCJ-deficient CD8 cells. Increased oxidative phosphorylation and subcellular ATP accumulation caused by the loss of MCJ selectively increase the secretion, but not the expression, of IFNγ. MCJ also serves to adapt effector CD8 T cell metabolism during the contraction phase. Consequently, memory CD8 cells lacking MCJ are superior in providing protection against influenza virus infection. Thus, MCJ offers a novel mechanism for fine-tuning mitochondrial metabolism in CD8 cells, as an alternative to modulating mitochondrial mass, which is an energetically expensive process. MCJ could be a new therapeutic target to enhance CD8 cell responses.

*Corresponding author: Mercedes Rincon, Ph.D., Professor, Department of Medicine/Immunbiology Program, Given C331, University of Vermont, 89 Beaumont Ave, Burlington, VT 05405.

INTRODUCTION

Metabolism is emerging as a major factor that regulates the function and differentiation of immune cells and influences the course of an immune response (Pearce et al., 2013; van der Windt and Pearce, 2012; Wahl et al., 2012; Wang and Green, 2012). Antigen stimulation leads to rapid cell growth and clonal expansion and is accompanied by changes in cell metabolism. Naïve, effector and memory T cell subsets have distinct metabolic profiles to provide the energy and the bioenergetic precursors required. Naïve cells use glucose and free fatty acids (FFA) as the sources of ATP through mitochondrial oxidative phosphorylation (OXPHOS) (van der Windt et al., 2012; Wang et al., 2011). Following activation, CD8 cells undergo a reprograming of their metabolic pathways and switch to glycolysis as a source of ATP. Effector T cells can also use glutamine to generate ATP through glutaminolysis, which can further fuel OXPHOS in mitochondria (Carr et al., 2010; Wang et al., 2011). Proliferation of effector CD8 cells appears to be more dependent on glucose than effector CD4 cells (Frauwirth et al., 2002; Macintyre et al., 2011). In contrast to proliferation, production of some cytokines by effector CD8 cells is not affected by a strong inhibition of glycolysis (Cham et al., 2008), and cytotoxic activity can occur in the absence of glucose (MacDonald, 1977; MacDonald and Koch, 1977).

Effector CD8 cells further reprogram metabolism during the generation of memory cells in response to antigen and cytokine withdrawal. Memory CD8 cells primarily use FFA oxidation in mitochondria as the main energy pathway (Araki et al., 2009; Pearce et al., 2009; van der Windt et al., 2012). Additionally, memory CD8 cells manifest a greater increase in both OXPHOS and aerobic glycolysis following activation compared with naïve cells, and the induction of glycolysis is dependent on mitochondrial ATP (van der Windt et al., 2013). Importantly, intervention of metabolism with metformin (AMPK activator) or rapamycin (mTOR inhibitor) to promote FFA oxidation enhances the generation of memory CD8 cells and protection against viral infection (Araki et al., 2009; Pearce et al., 2009). A recent study has revealed that memory CD8 cells have developed their own intrinsic pathways to mobilize fatty acids that are then used for fatty acid oxidation (Pearce et al., 2009). Considering this highly dynamic metabolic reprogramming, CD8 cells likely utilize specific checkpoints to regulate these transitions and their effector functions. However, while a number of studies have addressed the effect of different metabolic substrates that feed into the mitochondrial electron transfer chain (ETC), little is known about endogenous mechanisms that control mitochondrial respiration and, thereby, the immune response.

Methylation-Controlled J protein (MCJ/DnaJC15) is a member of the DnaJ family of chaperones. MCJ is a small protein with features that distinguish it from other DnaJC family members. While most DnaJC family members are soluble proteins, MCJ contains a transmembrane domain and has a unique N-terminal domain that shares no significant sequence similarity with any other known protein. MCJ was first reported in ovarian cancer cell lines and ovarian tumors as a gene negatively regulated by methylation (Shridhar et al., 2001; Strathdee et al., 2004). Loss of MCJ has been associated with chemoresistance of human breast and ovarian cancer cell lines *in vitro* (Hatle et al., 2007b), (Shridhar et al., 2001), and *in vivo* (Strathdee et al., 2005). We have recently shown that MCJ is abundantly expressed primarily in tissues with a highly active mitochondrial metabolism, including

heart and liver (Hatle et al., 2013). Within the immune system, MCJ is highly expressed in CD8 cells, but not in CD4 and B cells (Hatle et al., 2013), and it is also expressed in macrophages although at lower levels (Navasa et al., 2015a). Importantly, MCJ localizes to the inner membrane of mitochondria (Hatle et al., 2013; Schusdziarra et al., 2013). MCJ acts as a negative regulator of the ETC and MCJ deficiency *in vivo* results in increased Complex I activity and mitochondrial membrane potential (MMP) without affecting mitochondrial mass (Hatle et al., 2013). Endogenous MCJ in primary tissues associates with Complex I and acts as a natural inhibitor, making MCJ one of the first described endogenous negative regulators of Complex I. The activity of Complex I is enhanced by its assembly in "respirasomes" which are mitochondrial ETC supercomplexes containing Complexes I, III, and IV (Acin-Perez et al., 2008; Althoff et al., 2011). The function of these supercomplexes is to facilitate efficient transfer of electrons between these complexes to enhance Complex I activity and minimize the risk of electron "leak" that results in ROS production (Chen et al., 2012; Moreno-Lastres et al., 2012; Vukotic et al., 2012). We have shown that MCJ interferes with the formation of these supercomplexes (Hatle et al., 2013), a mechanism to inhibit Complex I activity and MMP. MCJ deficiency leads to enhanced mitochondrial activity which results in increased lipid metabolism in the liver and prevents the development of liver steatosis caused by starvation or by feeding with a high-cholesterol diet (Hatle et al., 2013). Thus, MCJ is a powerful negative regulator of metabolism in the liver.

Although MCJ is abundantly present in CD8 cells, its role in regulating mitochondrial metabolism and function of these cells is unknown. In this study, we show that MCJ acts a negative regulator of mitochondrial respiration in CD8 cells. MCJ deficiency does not affect proliferation of naïve CD8 cells upon activation, activation markers or cytokine gene expression. However, increased OXPHOS in MCJ deficient CD8 cells enhances the secretion of cytokines, and sustains the metabolic state of CD8 cells during the contraction phase of effector CD8 cells. Importantly, MCJ deficient memory CD8 cells have greater protective capacity against influenza virus infection. MCJ is therefore emerging as an important negative regulator of mitochondrial activity of CD8 cells.

RESULTS

Loss of MCJ promotes respiratory supercomplexes and mitochondrial metabolism in naïve CD8 cells

MCJ is as an endogenous inhibitor of mitochondrial Complex I and mitochondrial membrane potential (MMP) that is abundantly expressed in CD8 cells where it contributes to the maintenance of their mitochondria in a hypopolarized state (Hatle et al., 2013). However, the role of MCJ in CD8 cell development and function remains unknown. To investigate this, we used MCJ knockout (KO) mice previously described to have no obvious phenotypic alterations under physiological conditions (Hatle et al., 2013). Although CD8 cells freshly isolated from MCJ KO mice display higher mitochondrial membrane potential (MMP) (Supplementary Fig. S1A), there was no difference in the percentage (Supplementary Fig. S1B) and number (data not shown) of either CD8 or CD4 cells in the spleen and lymph nodes between MCJ KO and wildtype (WT) mice. No difference in the expression of activation markers such as CD44 was observed in either CD8 or CD4 cells freshly isolated

from spleen or lymph nodes (Supplementary Fig. S1C). In addition, the percentage (Supplementary Fig. S1B) and numbers (data not shown) of single CD8, single CD4, double positive (DP), and double negative (DN) populations in the thymus were comparable between MCJ KO and WT mice. Thus, MCJ deficiency does not affect the development of CD8 and CD4 cells in the thymus or homeostasis of cells in the periphery.

Mitochondrial membrane potential (MMP) is the driver for oxidative phosphorylation (OXPHOS), generation of ATP, and oxygen consumption. To investigate the impact that the increased MMP in CD8 cells from MCJ KO mice has on mitochondrial respiration, we examined the oxygen consumption rate (OCR) in freshly isolated WT and MCJ KO CD8 cells using the Seahorse MitoStress assay. Correlating with the increased MMP, OCR was also elevated in MCJ KO CD8 cells relative to WT CD8 cells (Fig. 1A). In contrast, the extracellular acidification rate (Pene et al.), a parameter for glycolysis, was not affected in MCJ KO CD8 cells (Fig. 1B). We also examined mitochondrial ATP production determined by subtracting the OCR in the presence of oligomycin (the inhibitor of Complex V/ATP Synthase) from the OCR at baseline. Mitochondrial ATP production (ATP-linked OCR) was also higher in MCJ KO CD8 cells relative to WT CD8 cells (Fig. 1C). Thus, MCJ is a negative regulator of mitochondrial respiration in CD8 cells.

Since no obvious phenotypic difference could be detected by activation or differentiation markers between CD8 cells from WT and MCJ KO mice despite their higher mitochondrial respiration, we performed nonbiased high-throughput metabolic profiling to identify the impact of MCJ on the overall metabolism of naïve CD8 cells. Metabolome analysis in CD8 cells freshly isolated from WT and MCJ KO mice showed a large number of metabolic intermediates from different pathways equally present in both. However, there was a significant increase in the levels of some of the amino acids in MCJ KO CD8 cells relative to WT CD8 cells (Supplementary Fig. S2 and Supplementary Table 1). Interestingly, further statistical analysis revealed that most of the amino acids that were significantly elevated in MCJ KO CD8 cells belong to the essential amino acid group (Fig. 1D). In contrast, only the levels of tyrosine in the conditionally essential amino acid group, and asparagine in the non-essential group were significantly increased (Fig. 1D).

The preferential accumulation of amino acids that cannot be synthesized and need to be imported suggested that a greater level of amino acid transport occurred in MCJ KO CD8 cells compared with WT CD8 cells. Since amino acid transport is highly dependent on ATP, increased mitochondrial OXPHOS in the absence of MCJ could be responsible for this transport. To investigate the amino acid uptake capacity, freshly isolated CD8 cells from WT and MCJ KO mice were incubated in culture medium. After 16 h, supernatants were harvested and analyzed for their metabolic profile to determine the consumption of amino acids. Consistent with the increased amino acid levels in MCJ KO CD8 cells, the levels of several amino acids were significantly reduced in the culture supernatant of MCJ KO CD8 cells (Fig. 1E). In addition, metabolic flux analyses with ^{13}C and ^{15}N labeled amino acids showed increased uptake of extracellular glutamine by freshly isolated MCJ KO CD8 cells compared with WT CD8 cells (Supplementary Fig. S3A). Thus, the increased mitochondrial respiration resulting from MCJ deficiency in naïve CD8 cells *in vivo* promotes the uptake of amino acids.

The other metabolite that was significantly increased in MCJ KO CD8 cells relative to WT CD8 cells was succinate (Fig. 1F, Supplementary Fig. S2, and Supplementary Table 1), which is oxidized to fumarate by succinate dehydrogenase (ETC Complex II) in the TCA cycle in mitochondria. However, the levels of fumarate and the other components of the TCA cycle were not different (Fig. 1F). These results suggested that the elevated levels of succinate in MCJ KO CD8 cells were the result of impaired Complex II activity in MCJ KO CD8 cells. Using a Seahorse Extracellular Flux analyzer, we examined Complex II activity by determining OCR in response to succinate, the substrate of Complex II, as previously described (Salabei et al., 2014). Reduced Complex II activity was found in freshly isolated MCJ KO CD8 cells relative to WT CD8 cells (Fig. 1G). In addition, metabolic flux analyses where freshly isolated CD8 cells were incubated with [^{13}C, ^{15}N]-glutamine, an amino acid precursor of succinate (Supplementary Fig. S3B) revealed significantly higher levels of newly synthesized succinate in MCJ KO CD8 cells compared to WT CD8 cells (Fig. 1H). However, the levels of fumarate, the product of Complex II, were not increased in MCJ KO CD8 cells (Fig. 1H). Thus, Complex II appears to be uncoupled from the rest of the ETC in MCJ KO CD8 cells.

We have shown that the absence of MCJ in heart favors the accumulation of mitochondrial respiratory supercomplexes (Hatle et al., 2013), which are formed by the association of Complexes I, III, and IV, but exclude Complex II. Sequestration of Complex III in supercomplexes could then compromise Complex II activity. We therefore investigated whether the lack of MCJ could also facilitate the formation of supercomplexes in naïve CD8 cells. Mitochondrial extracts were generated from WT and MCJ KO CD8 cells in the presence of digitonin to preserve supercomplexes and resolved by blue native electrophoresis (Bourillot et al.). As a positive control, we used mitochondrial extracts from heart, as supercomplexes are abundantly present in these cells (Supplementary Fig. 3C). The supercomplex region was excised from the blue native gel, resolved by denaturing electrophoresis, and analyzed by Western blot for subunits of Complexes I (NDUFA9) and IV (CoxIV). The amount of supercomplexes as determined by the levels of each subunit in the supercomplex region were remarkably higher in MCJ KO CD8 cells compared with those in WT CD8 cells (Fig. 1I). As a control, analysis of CoxIV in the monomeric Complex IV region showed comparable levels in both WT and MCJ KO CD8 cells (Fig. 1I). To further support the accumulation of supercomplexes in MCJ KO CD8 cells, mitochondrial extracts were resolved by BNE, transferred to PVDF membrane, and analyzed by Western blot for subunits of Complexes I (NDUFA9) and III (Core1). Similar to the results previously obtained, increased NDUFA9 levels were present in the supercomplex region in MCJ KO CD8 cells, while the levels of NDUFA9 in the monomeric Complex I region were comparable between MCJ KO and WT cells (Fig. 1J). Similar results were obtained for Core1, a Complex III subunit (Fig. 1J). Thus, loss of MCJ promotes the formation of respiratory supercomplexes in naïve CD8 cells, in correlation with their increased MMP. Uncoupling Complex III from Complex II could cause the observed accumulation of succinate. Together, these results indicated that the function of MCJ in naïve CD8 cells is to restrict mitochondrial metabolism, and a deficiency in MCJ alters normal mitochondrial metabolism.

MCJ deficiency does not affect proliferation, but enhances the secretion of cytokines in activated CD8 cells

Although naïve CD8 cells primarily use mitochondrial respiration, upon activation they switch the metabolic machinery and use aerobic glycolysis as the primary source of energy for cell expansion (Caro-Maldonado et al., 2012; Krauss et al., 2001; Rathmell et al., 2000). We therefore investigated whether the enhanced mitochondrial metabolism found in MCJ KO CD8 cells could alter proliferation. Freshly isolated CD8 cells from WT and MCJ KO mice were stained with CFSE, activated with anti-CD3 and anti-CD28 antibodies (Abs), and proliferation was analyzed by flow cytometry. No differences were observed in the frequency of proliferating cells nor the number of cell divisions between MCJ KO and WT CD8 cells (Fig. 2A). Similar results were obtained measuring proliferation by [^{3}H]-thymidine incorporation (data not shown). Moreover, analysis of viability showed no difference in survival of MCJ KO CD8 cells after 2 days of activation (Fig. 2B). Expression of the cell surface activation markers CD69 and CD25 was similarly upregulated upon activation in WT and MCJ KO CD8 cells (Fig. 2C). In contrast, activated MCJ KO CD8 cells produced substantially higher levels of IFNγ (Fig. 2D) and IL-2 (Fig. 2E) compared with WT CD8 cells, as determined by ELISA. Thus, loss of MCJ does not interfere with activation or expansion of CD8 cells, but results in a greater production of cytokines.

Production of cytokines by CD8 cells upon activation is primarily regulated at the level of gene expression either by transcription or by mRNA stability. To address whether the increased levels of IFNγ detected in the culture supernatants from activated MCJ KO CD8 cells were caused by increased gene expression, we examined cytokine mRNA levels by quantitative RT-PCR. Surprisingly, despite the elevated levels of IFN and IL-2 as determined by ELISA, the levels of mRNA were not increased in activated MCJ KO CD8 cells compared with WT CD8 cells (Fig. 2F). Thus, MCJ had no effect on cytokine gene expression in CD8 cells. A recent study reported that aerobic glycolysis promotes IFNγ production at the translational level in effector CD4 cells (Chang et al., 2013). We therefore examined the levels of IFNγ in CD8 cells by intracellular staining and flow cytometry analysis. However, no difference in the intracellular levels of IFNγ was found between WT and MCJ KO CD8 cells (Fig. 2G). Similarly, although low levels of IL-2 were detected by intracellular staining, there was no difference between WT and MCJ KO CD8 cells (Fig. 2G). Thus, the increased levels of cytokines in MCJ KO CD8 cell supernatants were not due to significantly increased gene or protein expression.

Secretion of cytokines is another mechanism that regulates the overall levels of cytokines being produced, although little is known about the pathways involved. To investigate whether the increased levels of IFNγ detected in the supernatants of MCJ KO CD8 cells were caused by an enhanced secretion, WT and MCJ KO CD8 cells were activated with anti-CD3 and anti-CD28 Abs for 2 days, washed, resuspended, and equal numbers of cells were then incubated in medium alone without any additional stimulus for different periods of time. Higher levels of IFNγ were detected by ELISA in the supernatants from MCJ KO CD8 cells relative to WT CD8 cells at 2 h (Fig. 2H). IFNγ levels from MCJ KO CD8 cells continued increasing for at least 4 h and then remained constant, while the amount secreted by WT CD8 cells did not increase (Fig. 2H). Treatment with cycloheximide (CHX), an

inhibitor of protein synthesis, did not affect the levels of IFNγ produced during this period (Supplementary Fig. S4A), although this concentration of CHX prevented new protein synthesis triggered by the activation of naïve CD8 cells (Supplementary Fig. S4B). These results further support that increased protein translation was, most likely, not the primary cause for enhanced production of IFNγ in MCJ KO CD8 cells. We also examined the levels of IL-2 and GM-CSF, other cytokines produced by CD8 cells. We found increased levels of both cytokines in the supernatant of MCJ KO CD8 cells after 4 h (Supplementary Fig. S4C), indicating that the effect of MCJ in secretion is not restricted to IFNγ. To further confirm the enhanced capacity of secretion by MCJ KO CD8 cells, we performed ELISpot assays for IFNγ. The number of spots with a larger area (high IFNγ producers) was increased in MCJ KO CD8 cells (Fig. 2I). Enhanced secretion should result in lower accumulation of intracellular IFNγ if no additional synthesis takes place. We therefore performed intracellular staining for IFNγ after cells were incubated in medium and found lower levels in MCJ KO CD8 cells after 1 h (Supplementary Fig. S4D). Together these results indicate that MCJ deficiency augments cytokine production primarily by promoting the cytokine secretion capacity of effector CD8 cells.

Local mitochondrial production of ATP in the absence of MCJ promotes cytokine secretion

Since the loss of MCJ in effector CD8 cells affected cytokine secretion, but not proliferation, expression of cytokine genes, or expression of activation markers, we used an unbiased metabolomics approach to investigate which metabolic pathways were regulated by MCJ in effector CD8 cells. Metabolic profiling was obtained from equal numbers of WT and MCJ KO CD8 cells after two days of activation and resting for 4 h. Interestingly, while no obvious phenotypic differences in terms of size or activation markers could be detected between the cell types, MCJ deficiency caused well-defined metabolic changes (Supplementary Fig. S5). Similar to naïve CD8 cells, the absence of MCJ in activated CD8 cells resulted in increased levels of amino acids, but this increase was not restricted to essential amino acids as in naïve cells (Fig. 3A and Supplementary Fig. S5). In addition, a number of intermediate metabolites of the TCA and urea cycle pathways, two of the main mitochondrial pathways (Supplementary Fig. S6), were among the most elevated components in activated MCJ KO CD8 cells relative to WT CD8 cells (Supplementary Fig. S5 and Table 2). Similar to naïve CD8 cells, the levels of succinate were also drastically increased in activated MCJ KO CD8 cells, but the levels of fumarate, malate, and 2-hydroxyglutarate were also higher (Fig. 3B). The levels of citrulline and arginosuccinate, components of the urea cycle (Supplementary Fig. S6), were increased in activated MCJ KO CD8 cells (Fig. 3C). Although there was no difference in proliferation, the nucleotide pathways were also upregulated in the absence of MCJ (Fig. 3D and Supplementary Fig. S5). Although nucleotide synthesis is primarily cytosolic, mitochondrial metabolic pathways also feed into the nucleotide synthesis pathways, while purine salvage reactions consume aspartate to produce fumarate and recover AMP upon deamination to IMP (Choi et al., 2012). Thus, an unbiased metabolic screening revealed increased mitochondrial activity in MCJ deficient effector CD8 cells.

Effector CD8 cells are primarily glycolytic and use ATP from glycolysis instead of mitochondrial OXPHOS as the major source of energy. The studies above indicate that the absence of MCJ enhances overall mitochondrial activity. This could lead either to increased total levels of ATP as a consequence of two parallel sources generating ATP or redistribution of ATP synthesis from cytosolic glycolysis to mitochondrial OXPHOS. We therefore examined intracellular ATP levels. WT and MCJ KO CD8 cells were activated for 2 d and then rested for 4 h. Higher levels of total ATP were present in MCJ KO CD8 cells relative to in WT CD8 cells (Fig. 4A). To determine whether the elevated levels of ATP could come from increased mitochondrial respiration in the absence of MCJ, we performed Seahorse MitoStress analysis in activated WT and MCJ KO CD8 cells. OCR was higher in activated MCJ KO CD8 cells relative to WT CD8 cells, as shown by the effect of oligomycin on baseline OCR (oxygen consumption by OXPHOS) (Fig. 4B). These data indicate that the rate of ATP synthesis by mitochondria was increased in the absence of MCJ. In contrast, analysis of the extracellular acidification rate (Pene et al.) in response to glucose showed no difference between the two cell types (Fig. 4C), indicating that glycolysis was not affected. Thus, loss of MCJ promotes mitochondrial respiration without altering the glycolytic rate of effector CD8 cells.

The normal rate of glycolysis as determined by ECAR analysis correlated with the normal rate of proliferation and gene expression observed in MCJ KO CD8 cells. While glycolysis-derived ATP represents the predominant source of energy and is sufficient for these processes in activated cells, mitochondrial derived ATP could be essential for other CD8 cell functions. Due to the dynamic characteristics of mitochondria, this organelle could provide a subcellular microenvironment rich in ATP without the need to raise total cytosolic ATP levels. We investigated the presence of ATP-rich microdomains within activated CD8 cells using a previously described fluorescent probe that has been used to identify ATP/ADP intracellular accumulation (Rao et al., 2012). Confocal microscopy of live cells showed only a few punctate ATP probe accumulations in activated WT CD8 cells (Fig. 4D), while ATP puncta were abundant and prominent in MCJ KO CD8 cells (Fig. 4D). The subcellular ATP accumulations in MCJ KO CD8 cells represented the mitochondrial-derived ATP pool since treatment with oligomycin prevented their formation (Supplementary Fig. S7A). Moreover, co-staining of CD8 cells with the ATP probe in combination with Mitotracker, a mitochondrial marker, revealed colocalization of the ATP puncta with mitochondria in activated MCJ KO CD8 cells (Fig. 4E). Thus, MCJ deficiency facilitates the formation of ATP-rich microdomains within activated CD8 cells.

Most mechanisms of secretion are highly dependent on ATP (Jitrapakdee et al., 2010; Wiederkehr and Wollheim, 2006), therefore the formation of ATP-rich microdomains at specific subcellular localizations could facilitate increased secretion of cytokines. To address whether the increased secretion of IFNγ found in MCJ KO CD8 cells was mediated by the increased production of mitochondrial ATP, CD8 cells were activated for 2 d, treated with oligomycin during the last 4 h of activation, harvested, and incubated at equal numbers in medium alone for another 4 h. IFNγ levels in the supernatant were determined by ELISA. Inhibition of mitochondrial ATP synthesis by oligomycin suppressed the enhanced secretion of IFNγ by MCJ KO CD8 cells to WT levels (Fig. 4F). In contrast, oligomycin did not reduce, but increased the intracellular levels of IFNγ, as determined by intracellular staining

and flow cytometry (Supplementary Fig. 7B). Thus, MCJ acts as an endogenous negative regulator of mitochondrial respiration to restrict the production of mitochondrial ATP and secretion of cytokines such as IFNγ.

MCJ attenuates mitochondrial metabolism during the contraction phase of effector CD8 cells *in vivo*

A number of studies have shown that CD8 cells reprogram their mitochondrial metabolism during their differentiation from naïve to effector and from effector to memory stages (Pearce et al., 2013; van der Windt and Pearce, 2012; Wahl et al., 2012; Wang and Green, 2012). Memory CD8 cells also have greater mitochondrial mass and maximum respiratory capacity (van der Windt et al., 2012). OXPHOS has been shown to promote both the generation and expansion of memory CD8 cells (van der Windt et al., 2013), suggesting the presence of a potential mechanism to attenuate mitochondria and contain the expansion and effector function of memory cells. Since MCJ acts as an internal break for mitochondrial function in tissues with a high content of active mitochondria, we hypothesized that MCJ expression could be regulated during the contraction phase of effector CD8 cells as part of their metabolic reprograming. To examine MCJ expression in individual cells we used MCJ KO mice as they contain the β-galactosidase reporter gene inserted in the MCJ locus. We performed β-galactosidase activity assays by flow cytometry analysis in CD8 cells that were freshly isolated, activated (effector), and rested in medium alone after activation (rested effector) to mimic the contraction phase of effector cells and development of memory cells. WT CD8 cells were used as negative control (lacking β-galactosidase) for flow cytometry analysis (Supplementary Fig. S8A). The frequency of MCJ expressing cells was dramatically decreased in effector CD8 cells relative to naïve CD8 cells (Fig. 5A). We have recently shown that Ikaros, a transcriptional repressor known to attenuate gene expression (John and Ward, 2011), binds to the *MCJ* gene in macrophages to silence MCJ expression (Navasa et al., 2015b). Since Ikaros has been previously reported in CD8 cells (O'Brien et al., 2014) we performed chromatin immunoprecipitation analysis (ChIP) to determine whether Ikaros also binds the MCJ promoter in WT CD8 cells. Relative to naïve WT CD8 cells, greater Ikaros binding to the MCJ gene was found in activated WT CD8 cells (Fig. 5B). To determine whether MCJ downregulation might be needed for optimal IFNγ production by effector CD8 cells, we performed retroviral transduction for MCJ in WT CD8 cells activated for 40 h to reconstitute MCJ levels. Although the frequency of transduction was low (<15%) there was a significant reduction in the levels of IFNγ in WT CD8 cells transduced with an MCJ-expressing retrovirus relative to those transduced with an empty retrovirus (Supplementary Fig. S8B), suggesting that MCJ is present in naïve CD8 cells as an additional checkpoint to restrict potential effector function.

Interestingly, the frequency of CD8 cells expressing MCJ increased again when effector cells were rested in the presence of medium without additional stimuli (Fig. 5A). During the contraction phase, effector CD8 cells modulate their metabolism, become smaller, less active, and most of them die except for a few that survive to become memory T cells. We examined whether the observed re-acquisition of MCJ in resting effector CD8 cells contributed to the attenuation of metabolism and/or cell survival *in vitro* during the contraction phase. WT and MCJ KO CD8 cells were activated for 2 d, washed, and then

incubated in medium alone (without addition of cytokines) for different periods of time. After 24 h resting, most WT and MCJ KO CD8 cells remained alive (Fig. 5C). However, after 48 h only a few WT CD8 cells remained alive, while many MCJ KO CD8 cells were still viable even at 72 h (Fig. 5C). In addition, the surviving MCJ KO CD8 cells maintain the "blastic cell stage" (large) reminiscent of effector cells (data not shown). Analysis of MMP in live cells after 48 h of resting showed that a high proportion of WT CD8 cells had low MMP (Fig. 5D), similar to naïve CD8 cells (Supplementary Fig. S1A). In contrast, a large fraction of rested effector MCJ KO CD8 cells displayed high MMP relative to WT cells (Fig. 5D). To determine whether the increased survival in rested MCJ KO CD8 cells *in vitro* was due their intrinsic metabolic state (high MMP) or due to increased levels of IL-2 that can promote cell expansion, a blocking anti-IL2 Ab was added during the resting period. No differences were detected in the survival of MCJ KO CD8 cells after blocking IL-2 (Supplementary Fig. S9A). Furthermore, the addition of small amounts of recombinant IL-2 during the resting period resulted in increased expansion of both WT and MCJ KO CD8 cells (Supplementary Fig. S9B). Thus, re-acquisition of MCJ in rested effector CD8 cells contributes to the reduction of mitochondrial activity, restoration of a quiescent metabolic state and fitness impairment of effector CD8 cells during the contraction phase *in vitro*.

To address the role of MCJ in the contraction phase of antigen-specific effector CD8 cells *in vivo*, MCJ KO mice were crossed with OT-I TCR transgenic mice which express a TCR that recognizes ovalbumin (Hogquist et al., 1994). MCJ deficiency did not affect the development of OT-I CD8 cells (Supplement Fig. S10A). Similar to polyclonal CD8 cells, naive MCJ-deficient OT-I CD8 cells also displayed high mitochondrial membrane potential relative to WT OT-I CD8 cells (Fig. 5E). CD8 cells were purified from OT-I and MCJ KO OT-I mice, activated for 2 days *in vitro*, and then further expanded for 3 days. An equal number of cells from each genotype were combined and co-transferred into the same WT recipient mice to ensure equal efficiency of the adoptive transfer for both genotypes (Fig. 5F). Two weeks later, the presence of donor cells in lymph nodes and spleen from the host mice was examined by flow cytometry using CD90.1/CD90.2 markers to identify the WT and MCJ KO OT-I CD8 populations (Supplementary Fig. S10B). Phenotypic characterization of the cells based on CD44 and CD62L (memory and homing markers, respectively), as well as KLRG1 and CD127 (markers that define subsets of long-lived effector and memory T cells (Jameson and Masopust, 2009; Kaech et al., 2003; Kaech and Wherry, 2007; Sallusto et al., 2004; Sarkar et al., 2008) did not show differences between WT and MCJ KO CD8 cells (Supplementary Fig. S10B). The overall percentage of cell recovery in both donors was comparable (data not shown). However, as determined by forward scatter (Fig. 5G), only a few WT OT-I CD8 cells showed a large blastic phenotype (Fig. 5H). In contrast, a greater fraction of MCJ KO OT-I CD8 cells displayed the large blastic phenotype (Fig. 5H). Thus, *in vivo* MCJ does not seem to contribute to cell survival, but it participates in the attenuation of metabolism during the transition from effector to rested effector cells.

MCJ deficiency enhances the antiviral protective activity of memory CD8 cells

Memory CD8 cells are believed to play an important role in protection against viral infection (La Gruta and Turner, 2014). Recent studies indicated that increased mitochondrial

respiration in CD8 cells results in increased memory activity (van der Windt et al., 2013). To investigate the role of MCJ in protective memory CD8 response, we used the influenza virus infection model. WT and MCJ KO mice were intranasally infected with a sublethal dose of influenza A/Puerto Rico/8/34 (PR8) H1N1 virus. As expected, based on the predominant role of innate immunity in primary infection with influenza virus, no significant differences were observed in weight loss and recovery (hallmark of disease) or survival between infected WT and MCJ KO mice during primary infection (Fig. 6A). Analysis of influenza NP-tetramer positive CD8 cells 2 weeks post-infection showed a similar frequency between infected WT and MCJ KO mice (Fig. 6B), indicating that the loss of MCJ does not affect the expansion of effector CD8 cells *in vivo* consistent with the *in vitro* studies. However, *ex vivo* analysis of IFNγ production by CD8 cells from the infected mice showed higher levels of IFNγ in the supernatants of MCJ KO CD8 cells relative to WT CD8 cells (Fig. 6C). Thus, in agreement with the increased cytokine secretion detected *in vitro* with anti-CD3/CD28 stimulation, MCJ deficiency also results in increased IFNγ production by effector CD8 cells *in vivo* during virus infection.

We then addressed whether the lack of MCJ could affect the development of memory CD8 cells. Analysis of influenza NP-tetramer positive CD8 cells 3 weeks post-infection showed a lower percentage relative to 2 weeks post-infection as expected, but there was no difference in the frequency between WT and MCJ KO mice (Supplementary Fig. S11A). Similarly, five weeks post-infection, the frequency of NP-tetramer positive cells was not higher in infected MCJ KO mice compared to WT mice (Fig. 6D), further supporting that lack of MCJ does not affect cell survival during the generation of memory CD8 cells from effector cells *in vivo*. Phenotypic analysis of these NP-tetramer positive CD8 cells for CD44, CD62L, KLRG1, and CD127 showed no substantial difference between WT and MCJ KO CD8 cells (Supplementary Fig. S11B and data not shown). Further analysis for CD27 expression revealed a slightly higher proportion of $KLRG^{-}CD127^{+}$ cells lacking CD27 and $KLRG^{+}CD127^{-}$ cells were largely $CD27^{low}$ (Supplementary Fig. S11B). Within the memory population, $CD27^{low}$ cells have been reported to mediate rapid protective immunity against acute infection and manifest high cytolytic activity (Olson et al., 2013)

To investigate the protective capacity of memory MCJ KO CD8 cells, we performed adoptive transfer of equal numbers of CD8 cells from WT and MCJ KO mice obtained five weeks post-infection into WT recipient mice. Recipient mice were then infected with a lethal dose of PR8 influenza virus. As expected, recipient mice that received purified CD8 cells from infected WT mice were not protected and died between 8–9 days post lethal infection (Fig. 6E). In contrast, most recipient mice that received purified CD8 cells from infected MCJ KO mice were protected against the lethal dose of PR8 influenza virus (Fig. 6E). Weight loss analysis showed that mice receiving MCJ KO CD8 cells indeed lost weight initially (Fig. 6F), indicating that they had been infected. However, these mice were able to recover their weight to healthy levels (Fig. 6F). Host mice that received WT CD8 cells did not recover their weight (Fig. 6F), correlating with their early death. Thus, the absence of MCJ in memory CD8 cells confers greater protective capacity against influenza virus infection.

Death caused by some of the highly pathogenic influenza virus such as H5N1 influenza virus is often associated with a strong systemic immune response and cytokine storm. To rule out that the death of WT CD8 cell recipient mice was caused by an exuberant immune response relative to the response in MCJ KO CD8 cell recipients, we examined cytokine production 6 days post-infection with the lethal dose. The levels of inflammatory cytokines (IL-6, KC) as well as chemokines (CXCL10) in brochoalveolar lavage fluid (BALF) were comparable in both cell type hosts (Fig. 6G). Similarly, the levels of these cytokines in serum (systemic) were also comparable (Supplementary Fig. S12A). These results indicated that the protection found in mice that received MCJ KO CD8 cells was not due to an attenuated immune response relative to mice with WT CD8 cells.

To investigate whether the protective capacity of memory MCJ KO CD8 cells was due to an improved effector function to clear virus, we examined PR8 influenza virus titers in the lung of recipient mice 6 days post-infection with a lethal dose of influenza virus. High virus titers were present in host mice that received WT CD8 cells (Fig. 6H). In contrast, significantly lower virus titers were present in the lungs from host mice that received MCJ KO CD8 cells (Fig. 6H). These data indicate that memory MCJ KO CD8 cells are more efficient in clearing influenza virus. To examine the effector function of the memory MCJ KO CD8 cells, CD8 cells were isolated from mediastinal lymph node (MLN) six days after lethal infection and *ex vivo* IFNγ was determined by culturing cells in medium alone. Increased levels of IFNγ were produced by MCJ KO CD8 cells relative to WT CD8 cells (Fig. 6I). The NP-tetramer positive frequency was not different in MLN (Supplementary Fig. S12B). Similarly, *ex vivo* IFNγ production by MCJ KO CD8 cells isolated from lung was also increased (Supplementary Fig. S12C). Furthermore, although there was no difference in the frequency of NP-tetramer positive CD8 cells from the lung between WT and MCJ KO mice (Supplementary Fig. S12D), the number of IFNγ-secreting cells as determined by ELISpot assay was also higher in MCJ KO CD8 cells (Fig. 6J).

Secretion of granules by exocytosis is a process dependent on both Ca^{2+} and ATP. We investigated whether increased mitochondrial ATP production in MCJ KO CD8 cells could also facilitate the exocytosis of the cytotoxic granules present in effector cells and contribute to their antiviral activity using a CD107a mobilization assay, which is a well-established approach to measure the release of granules (Gomperts, 1990). CD8 cells were isolated from the MLN of WT and MCJ KO mice 6 days post lethal infection and incubated in medium containing monensin with or without ionomycin to provide the Ca^{2+} signal. The frequency of $CD107a^{+}$ MCJ KO CD8 cells treated with ionomycin was significantly higher than WT CD8 cells (Fig. 6K), indicating that MCJ KO CD8 cells have a greater capacity to function as cytotoxic cells. Thus, increased mitochondrial respiration caused by the loss of MCJ in CD8 cells results in increased antiviral protective activity in memory responses by enhancing the secretion both of effector cytokines as well as cytotoxic granules.

DISCUSSION

Mitochondria play a key role in balancing cellular metabolism primarily, but not exclusively, as the site for OXPHOS through the ETC and as a source of ATP. Recently, it has become clear that tight regulation of mitochondrial metabolism occurs during the reprograming of

CD8 cells. OXPHOS is a complicated process that requires the presence of several ETC Complexes located in the inner membrane that are coupled with other enzymatic reactions that occur in the mitochondria matrix. In addition, ETC Complexes are orchestrated into respiratory supercomplexes to facilitate the electron transport. A number of molecules have been shown to be required for maximum efficiency of the ETC and OXPHOS. However, other than the availability of substrates (glucose, glutamine, FFA) that eventually feed into the ETC, very little is known about negative regulatory mechanisms that restrict mitochondrial respiration to avoid unnecessary use of the ETC. We have recently identified MCJ as one of the first known negative regulators of Complex I activity through its effect in the formation of respiratory supercomplexes (Hatle et al., 2013). Interestingly, MCJ is abundantly present in tissues with highly active mitochondrial metabolism including heart and liver, and is also highly expressed in CD8 cells. MCJ is only present in vertebrates (Hatle et al., 2007a), and was most likely acquired during evolution as a mechanism to attenuate mitochondrial metabolism as an alternative to mitochondria clearance. Our earlier studies demonstrated that the absence of MCJ during starvation prevents the development of fatty liver by accelerating fatty acid metabolism within the liver (Hatle et al., 2013). Here we show that MCJ restrains mitochondrial respiration in CD8 cells. In the absence of this natural break, CD8 cells have enhanced OXPHOS leading to increased secretion of cytokines by effector CD8 cells. In addition, MCJ deficiency interferes with the metabolic adaptation during the contraction phase of effector CD8 cells and results in greater antiviral protective activity of memory CD8 cells.

Effector and memory CD8 cells need ATP for effector functions in addition to cell growth and expansion. While CD8 cells primarily use glycolysis instead of OXPHOS for proliferation (Caro-Maldonado et al., 2012), other sources may provide the ATP required for processes that use high levels of ATP. In this regard, production of some cytokines by effector CD8 cells is not affected by strong inhibition of glycolysis (Cham et al., 2008), and cytotoxic activity can take place in the absence of glucose (MacDonald, 1977; MacDonald and Koch, 1977). Considering the dynamic aspect of mitochondria as organelles that can rapidly relocate in the cytosol, it is quite possible that mitochondria contribute to the synthesis of ATP for some of these processes. Mitochondria can create a microenvironment that is highly rich in ATP in specific locations (*e.g.*, near the cytosolic membranes), without elevating overall cytosolic ATP levels (a costly process). Mitochondria have been shown to relocate at the edge of lamellipodia and are critical to provide energy for migration of cells (Morlino et al., 2014). Our studies reveal the presence of microenvironments where ATP/ADP accumulate in CD8 cells that are located in the proximity of mitochondria. Thus, mitochondrial ATP could be used for specific purposes. Here we show that increased mitochondrial respiration in CD8 cells lacking MCJ has no effect on the proliferation of CD8 cells or cytokine gene expression, but it enhances the secretion of cytokines such as IFNγ. Little is known about the mechanisms of cytokine secretion in T cells, however secretion or release of intracellular components is highly dependent on ATP. In neurons, secretion through porosomes is also known to require high amounts of ATP (Jena, 2013). Secretion through transporters (*e.g.*, IL-1) is another mechanism with high ATP cost (Monteleone et al., 2015). Whether ATP in these secretions processes is derived from mitochondria or cytosolic ATP from glycolysis has yet to be determined. We show here that

secretion of IFNγ by CD8 cells in the absence of MCJ is dependent on ATP derived from mitochondria. Thus, mitochondria through OXPHOS can regulate effector function of CD8 cells independently of cell expansion.

The presence of respiratory supercomplexes in mammalian cells has been demonstrated in some of the tissues such as heart. Respirasomes (formed by Complexes I, III, and multiple units of Complex IV) bring the individual complexes together to facilitate the efficient transfer of electrons between complexes and prevent electron leaks. Thus, the formation of respiratory supercomplexes is a mechanism to minimize the production of ROS, which could be highly toxic for cells, primarily in those that need to proliferate. Here we reveal the presence of supercomplexes in naïve CD8 cells and increased supercomplex formation in the absence of MCJ as we previously showed for MCJ-deficient hearts (Hatle et al., 2013). Naïve CD8 cells use primarily mitochondria and OXPHOS relative to activated CD8 cells, however the levels of mitochondrial ROS are almost undetectable (Hatle et al., 2013). It is possible that the presence of supercomplexes prevents the formation of ROS and enhances survival of naïve cells. Normally, increased MMP is associated with increased ROS levels. Interestingly, while MMP is substantially increased in MCJ-deficient CD8 cells, the levels of ROS are not increased in naïve CD8 cells (Hatle et al., 2013) or they are even reduced in activated cells (Supplementary Fig. S13) compared with WT CD8 cells, correlating with the increased levels of supercomplexes. To date there is no clear evidence that Complex II (succinate dehydrogenase) is also recruited to supercomplexes. Since Complex III receives electrons from both Complex I and Complex II, the recruitment of Complex III to supercomplexes may cause an uncoupling of Complex III from Complex II. Therefore, Complex II activity may be attenuated to prevent electron leakage since its corresponding acceptor, Complex III, is sequestered. This could explain the accumulation of succinate in MCJ-deficient CD8 cells.

Memory CD8 cells utilize mitochondrial respiration for both their generation and effector function. Memory CD8 cells have greater spare respiratory capacity and use mitochondrial respiration as a primary source of energy (van der Windt et al., 2012; van der Windt et al., 2013; van der Windt and Pearce, 2012). However, instead of using glucose to feed mitochondrial respiration through pyruvate, memory CD8 cells perform β-oxidation of fatty acids. Recently, it has been shown that these cells utilize lipolysis to generate their own fuel (O'Sullivan et al., 2014). Pathways leading to increased mitochondrial respiration are associated with a superior memory CD8 response. A recent study has identified Lymphocyte Expansion Molecule (LEM) as a novel protein that promotes memory CD8 response by increasing OXPHOS indirectly by boosting the translation of proteins synthesized in the mitochondria (Okoye et al., 2015). In our study, we identify MCJ as an endogenous negative regulator of OXPHOS in CD8 cells. Lack of MCJ sustains the active metabolism of effector CD8 cells during the contraction phase and results in greater effector memory CD8 responses to influenza virus. Although MCJ deficiency has an impact in the metabolic adaptation during the contraction phase of effector CD8 cells, it does not seem to have a substantial effect on overall survival of those effector cells *in vivo,* based on the results from the adoptive transfer of effector OT-I cells as well as the influenza virus infection. MCJ deficiency appears to provide survival advantage to effector cells when these cells are rested in medium alone without additional cytokines *in vitro*. This is most likely due to the fact that

during *in vitro* resting effector WT CD8 cells undergo cytokine withdraw, while during the contraction phase *in vivo* the cytokine environment (e.g. IL-15, IL-2) can provide survival signals. Accordingly, addition of IL-2 during the resting period *in vitro* also promotes survival and expansion of WT CD8 cells. We also show here that WT memory CD8 cells alone fail to provide protection against a lethal dose of influenza virus. Strikingly, MCJ-deficient memory CD8 cells are highly protective against lethal infection with influenza. This is most likely due to the increased mitochondrial metabolism in those memory CD8 cells. Using the LCMV infection model, it has been shown that CD4 cells can rescue exhausted CD8 cells during chronic viral infection (Aubert et al., 2011). We also observed that a small frequency of CD4 cells is sufficient for WT memory CD8 cells to provide protection against influenza virus infection (data not shown). Since MCJ deficiency results in enhanced CD8 cell response, the question that remains is what is the evolutionary rationale for MCJ to be expressed in CD8 cells. While CD8 cells are key for protection, an exaggerated cytotoxic CD8 response could cause non-specific tissue damage particularly since CD8 cells recognize antigens presented by MHC class I, which is ubiquitously expressed (in contrast to MHC class II). We propose that MCJ was acquired in CD8 cells as a strategy to restrain CD8 cell metabolism and prevent a prolonged effector function that could be harmful.

In summary, we have identified MCJ as an endogenous regulator of mitochondrial respiration that serves as a break to avoid the overuse of mitochondrial metabolism and restrain CD8 cell responses. MCJ could therefore be a novel target to enhance CD8 responses during vaccination or immunotherapy. However, genetic loss of MCJ in CD8 cells may result in an unrestrained response that could contribute to autoimmune diseases. Alternatively, silencing MCJ expression in CD8 cells may be part of a promising immunotherapy approach in cancer treatment.

EXPERIMENTAL PROCEDURES

Mice

All mice were bred and maintained under specific pathogen free conditions at the University of Vermont animal care facility and used under procedures approved by the University of Vermont Institutional Animal Care and Use Committee. Mouse strains used were WT C57BL/6J (Jackson Laboratories), MCJ KO (Hatle et al., 2013), OT-I TCR transgenic (OT-I) (Hogquist et al., 1994), and MCJ KO x OT-I mice (OT-I KO).

Cell preparation and culture

CD8 cells were purified from spleen and lymph nodes (LN) by negative selection as previously described (Farley et al., 2006) and by positive selection using the MACS Cell Separation System (Miltenyi) as recommended by the manufacturer. The purity of isolated cells was confirmed by flow cytometry. Cells were activated *in vitro* using plate bound anti–CD3 (5 μg/mL) and soluble anti–CD28 (1 μg/mL) antibodies (BioXcell). For analysis of cytokine secretion during resting, cells were activated for 2 days, washed, and incubated at equal numbers in medium alone without additional stimuli for 4 – 12h. Culture supernatants of activated and rested cells were analyzed for IFNγ, IL-2, or GM-CSF by ELISA. Cells

were also incubated with or without oligomycin (20 μM, Sigma), or cycloheximide (5 μg/ml, Sigma). For cell survival analysis, activated cells were washed and incubated at equal numbers in medium without further stimulation or the presence of exogenous cytokines. In some cases, the culture medium was supplemented with anti-IL-2 Ab or recombinant IL-2 after 24 h. Live cells were determined by Trypan blue exclusion at 24, 48, and 72 h after replating.

Mitochondrial respiration and extracellular acidification

Oxygen consumption rates (OCR) of CD8 cells were analyzed under basal conditions and in response to sequential injections of oligomycin, FCCP, and rotenone with antimycin A (1 μM each) using the XF Cell Mito Stress Test Kit. Extracellular acidification rates (ECAR) were analyzed under basal conditions and in response to glucose (10mM) using the XF Cell Mito Stress Test Kit. OCR linked to mitochondrial ATP production (ATP-linked OCR) was determined by subtracting the OCR of CD8 cells reached after treatment with oligomycin from the OCR obtained at baseline. Complex II-linked respiration was determined using a modified version of a previously described method (Salabei et al., 2014). Briefly, XF24 cell culture microplates were coated with Cell-Tak (50uL at 22.4ug/mL, Corning) and freshly isolated CD8 cells were plated in MAS-BSA assay solution (220 mM mannitol, 70 mM sucrose, 10 mM KH_2PO_4, 5 mM $MgCl_2$, 2mM HEPES, 1 mM EGTA, 0.2% fatty acid free BSA) containing XF plasma membrane permeabilizer (PMP, 1nM, Seahorse Bioscience) and ADP (4mM, Sigma). Oxygen consumption rates were measured at baseline and in response to sequential injections of succinate (10mM, Sigma) with rotenone (2μM Seahorse Bioscience) and malonate (500 μM, Sigma) using an XF-24 Extracellular Flux Analyzer (Seahorse Bioscience) as recommended by the manufacturer.

Mass spectrometry based metabolomics

For metabolomics analyses, CD8 cells from WT and MCJ KO mice were purified and either left unstimulated or activated for 2 days prior to mass spectrometry analysis. For culture supernatants, unstimulated CD8 cells were incubated in medium without stimulation for 16 h. For heavy isotope and flux analyses, unstimulated cells were incubated in medium supplemented with Cell Free Amino Acid Mixture - ^{13}C, ^{15}N (2mM, Sigma) for 5 min or 5 h. Metabolomics and flux analyses were performed as previously reported (D'Alessandro et al., 2015). Briefly, 2×10^6 cells and 20 μl of cell media were extracted in 1 ml and 980 μl of cold lysis/extraction buffer (methanol:acetonitrile:water 5:3:2), respectively. After discarding protein pellets, 10 μl of water and methanol soluble fractions were run through a Kinetex C18 1.7 μm, 100 × 2.1 mm reversed phase column (phase A: water, 0.1% formic acid; B: acetonitrile, 0.1% formic acid; Phenomenex) via an ultra-high performance chromatographic system (UHPLC - Ultimate 3000, Thermo Fisher). UHPLC was coupled in line with a high resolution quadrupole Orbitrap instrument run in both polarity modes (QExactive, Thermo Fisher) at 140,000 resolution (at 200 m/z). Metabolite assignment, heavy isotopologue distributions and peak integration for relative quantitation were performed through the software Maven (Princeton), against the KEGG pathway database and an in-house validated standard library (>650 compounds, Sigma Aldrich, IROATech). Integrated peak areas were exported to Excel (Microsoft) and elaborated for statistical analysis (*t* test, ANOVA) and

hierarchical clustering analysis (HCA) through Prism (GraphPad Software) and GENE-E (Broad Institute), respectively.

Mitochondrial respiratory supercomplexes

Mitochondrial fractions were obtained by differential centrifugation, solubilized with 2% digitonin (Sigma), and resolved by electrophoresis using NativePAGE Novex 4–16% Bis-Tris protein gels (Invitrogen) as previously described (Hatle et al., 2013; Yang et al., 2015). Bands corresponding to respiratory supercomplexes and monomeric Complex IV were excised from the Blue Native gel, eluted, resolved by SDS-PAGE, and analyzed by Western blot for NDUFA9 and CoxIV (MitoScience). Proteins were also transferred directly from the Blue Native gel to PVDF membrane for Western blot analysis for NDUFA9 and Core1 (MitoScience).

Intracellular ATP Concentration

Intracellular ATP concentration in CD8 cells (10^4) was determined using the ATPlite Luminescence Assay System (PerkinElmer) and a TD-20/20 Luminometer (Turner BioSystems) as recommended by the manufacturers.

Flow cytometry analyses

For cell proliferation analysis, cells were stained with CFSE (250 μM, Molecular Probes), activated for 24 or 48 h, and examined by flow cytometry analysis to determine proliferation. Control (unstimulated) cells were stained and incubated in medium alone for 16 h before analysis. For cell survival analysis, cells were stained using the Live/Dead Cell Viability Assay (Molecular Probes) as recommended by the manufacturer and examined by flow cytometry analysis. For expression of cell surface markers, cells were stained with antibodies for CD4, CD8, CD25, and CD69, and then analyzed by flow cytometry. For mitochondrial membrane potential analysis, cells were staining with TMRE (Molecular Probes) as previously described (Hatle et al., 2013) and examined by flow cytometry analysis. For β-galactosidase activity analysis, cells were incubated in β-galactosidase substrate (FACS Fluorescent Blue lacZ β-Galactosidase Detection Kit, Marker Gene Technologies) as recommended by the manufacturer and analyzed by flow cytometry. WT cells were used as negative controls. For intracellular cytokine staining analysis, cells were fixed after activation in paraformaldehyde, permeabilized with saponin and stained with the corresponding antibodies for IFNγ or IL-2 (BD Bioscience) as previously described (Yang et al., 1998). No pre-incubation with brefeldin A or monensin was used prior to intracellular staining. For CD107a mobilization assay, cells were cultured in the presence of monensin (1 μM, Sigma) and anti-CD107a (4 μL/ml, Biolegend) for 4 h using a modified version of a previously described method (McElroy et al., 2007). Additionally, cells were cultured with or without ionomycin (250ng/ml). Cells cultured without anti-CD107a were used as negative controls. All flow cytometry analyses were performed using an LSRII Flow Cytometer (BD Biosciences) and FlowJo software.

Cytokine Analyses

For cytokine gene expression analysis, total RNA was isolated from activated cells using an RNeasy Mini Kit (Qiagen) as recommended by the manufacturer, cDNA was synthesized as previously described (Yang et al., 2015), and mRNA levels for IL-2 and IFN were determined by qRT-PCR using Assays–on–Demand TaqMan Gene Expression Assays (Applied Biosystems). Values were normalized to β_2–microglobulin and analyzed by the comparative delta CT method. For cytokine production analysis, IFNγ and IL-2 levels in culture supernatants were determined by ELISA as previously described (Yang et al., 1998). For IFNγ ELISpot assays, cells were washed and plated in an ELISpot assay plate using a capture and biotinylated anti-IFNγ Abs (MabTech). ELISpot assay was performed as previously described (Dienz et al., 2009). Total and larger spots (high IFNγ–producing cells) were quantified using an Axio Imager and software system (Zeiss).

Chromatin immunoprecipitation

Ten to fifteen million purified CD8 cells were activated for 2 days or left unstimulated. ChIP assays were performed as previously described (Navasa et al., 2015b) using the SimpleChip Enzymatic Chromatin IP kit-Magnetic beads (Cell Signaling) following the manufacturer's instructions using anti-Ikaros or normal rabbit IgG as a negative control. Immunoprecipitated DNA was subjected to q-PCR using primers encompassing the Ikaros binding site (5′-TCA TTT GCT GTG AGC GCA AG-3′ and 5′-GCC TCC TTA GGT CTA CCT TGA-3′). Results are presented as fold induction over rabbit IgG immunoprecipitates relative to input (percent input method).

Influenza infection and analyses

WT and MCJ KO mice were infected intranasally with a sublethal dose (3×10^3 EIU) of Puerto Rico A/PR/8/34 H1N1 influenza A (PR8) virus as previously described (Dienz et al., 2012). Mice were monitored for weight loss every other day. CD8 cells were isolated by positive selection from the draining mediastinal lymph node (MLN) and spleen five weeks later. Equal numbers of NP tetramer positive CD8 cells ($2–2.5\times10^6$) were then transferred to WT mice, and a day later recipient mice were infected with a lethal dose of PR8 virus (10^4 EIU). Mice were monitored for weight loss every other day. Animals that lost >30% of their body weight at the day of infection or became grossly moribund were euthanized. BALF and serum were collected 6 days after the lethal dose. Cytokines and chemokines in BALF and serum were examined using Luminex Mouse cytokine/chemokine panel I (Millipore) according to the manufacturer's protocol. *Ex vivo* production of IFNγ by CD8 cells from the MLN and lung were determined by ELISA and/or ELISpot assay as described above. CD8 cells were also stained with $NP_{366–374}/D^b$ tetramers containing peptide from the PR8 influenza virus (Powell et al., 2007), and antibodies for CD44, CD62L, KLRG1, CD127, and CD27 (Biolegend) and analyzed by flow cytometry. For virus copy determination, total RNA extracted from whole lung tissue by RNeasy Kit (Qiagen) was used for cDNA synthesis (2 μg of RNA) as previously described (Dienz et al., 2012). Viral titers were determined by real-time RT-PCR for PR8 virus acid polymerase (PA) gene, a method validated as equivalent to PFU (Jelley-Gibbs et al., 2007).

Confocal microscopy

Cells were activated for 2 d, transferred to glass bottom plates (MatTek), and incubated at 37°C for 1 h to sediment. Live cells were examined by confocal microscopy prior to the addition of the probe (background). ATP probe (Rao et al., 2012) was then added (100 μM), cells were incubated for 5 min, washed, and visualized using a 405nm laser. For co-staining with Mitotracker, prior to incubation with the ATP probe cells were incubated with Mitotracker (Thermo Fisher) for 30 min. Confocal microscopy performed using a Zeiss LSM 510 Meta Confocal Laser Scanning microscope (Carl Zeiss Microscopy).

Statistical analyses

Statistical significance was determined by *t* test or one-way ANOVA in cases where more than two groups were analyzed. Bars represent the mean with the standard deviation (SD) or standard error of the mean (SEM). Kaplan-Meier survival curves were analyzed using the log-rank test. $p < 0.05$ was considered statistically significant.

Supplementary Material

Refer to Web version on PubMed Central for supplementary material.

Acknowledgments

We thank T. Hunter and J. Hoffman for help with qRT–PCR analysis (DNA Analysis Facility, Univ. of Vermont), R. del Rio-Guerra for help with flow cytometry analysis (Flow Cytometry and Cell Sorting Facility, Univ. of Vermont), N. Bouffard for help with confocal microscopy (Microscopy Imaging Center, Univ. of Vermont), Estibaliz Atondo and Itziar Martín-Ruiz for help with the CHIP Assays (CIC bioGUNE), and P. Gummadidala and B. Silverstrim for technical support. This work was supported by the NIH grants AI110016 (M.R.) and P20 GM103496 (M.R. and K.H.). J.A. was partially funded by the Spanish Ministry of Economy Plan Nacional grant SAF2012-34610. R.Y. was supported through the American Association of Immunologists Careers in Immunology Fellowship Program.

References

Acin-Perez R, Fernandez-Silva P, Peleato ML, Perez-Martos A, Enriquez JA. Respiratory active mitochondrial supercomplexes. Mol Cell. 2008; 32:529–539. [PubMed: 19026783]

Althoff T, Mills DJ, Popot JL, Kuhlbrandt W. Arrangement of electron transport chain components in bovine mitochondrial supercomplex I1III2IV1. Embo J. 2011; 30:4652–4664. [PubMed: 21909073]

Araki K, Turner AP, Shaffer VO, Gangappa S, Keller SA, Bachmann MF, Larsen CP, Ahmed R. mTOR regulates memory CD8 T-cell differentiation. Nature. 2009; 460:108–112. [PubMed: 19543266]

Aubert RD, Kamphorst AO, Sarkar S, Vezys V, Ha SJ, Barber DL, Ye L, Sharpe AH, Freeman GJ, Ahmed R. Antigen-specific CD4 T-cell help rescues exhausted CD8 T cells during chronic viral infection. Proc Natl Acad Sci U S A. 2011; 108:21182–21187. [PubMed: 22160724]

Bourillot PY, Aksoy I, Schreiber V, Wianny F, Schulz H, Hummel O, Hubner N, Savatier P. Novel STAT3 target genes exert distinct roles in the inhibition of mesoderm and endoderm differentiation in cooperation with Nanog. Stem cells. 2009; 27:1760–1771. [PubMed: 19544440]

Caro-Maldonado A, Gerriets VA, Rathmell JC. Matched and mismatched metabolic fuels in lymphocyte function. Semin Immunol. 2012; 24:405–413. [PubMed: 23290889]

Carr EL, Kelman A, Wu GS, Gopaul R, Senkevitch E, Aghvanyan A, Turay AM, Frauwirth KA. Glutamine uptake and metabolism are coordinately regulated by ERK/MAPK during T lymphocyte activation. J Immunol. 2010; 185:1037–1044. [PubMed: 20554958]

Cham CM, Driessens G, O'Keefe JP, Gajewski TF. Glucose deprivation inhibits multiple key gene expression events and effector functions in CD8+ T cells. Eur J Immunol. 2008; 38:2438–2450. [PubMed: 18792400]

Chang CH, Curtis JD, Maggi LB Jr, Faubert B, Villarino AV, O'Sullivan D, Huang SC, van der Windt GJ, Blagih J, Qiu J, et al. Posttranscriptional control of T cell effector function by aerobic glycolysis. Cell. 2013; 153:1239–1251. [PubMed: 23746840]

Chen YC, Taylor EB, Dephoure N, Heo JM, Tonhato A, Papandreou I, Nath N, Denko NC, Gygi SP, Rutter J. Identification of a protein mediating respiratory supercomplex stability. Cell Metab. 2012; 15:348–360. [PubMed: 22405070]

Choi O, Heathcote DA, Ho KK, Muller PJ, Ghani H, Lam EW, Ashton-Rickardt PG, Rutschmann S. A deficiency in nucleoside salvage impairs murine lymphocyte development, homeostasis, and survival. J Immunol. 2012; 188:3920–3927. [PubMed: 22407915]

D'Alessandro A, Nemkov T, Kelher M, West FB, Schwindt RK, Banerjee A, Moore EE, Silliman CC, Hansen KC. Routine storage of red blood cell (RBC) units in additive solution-3: a comprehensive investigation of the RBC metabolome. Transfusion. 2015; 55:1155–1168. [PubMed: 25556331]

Dienz O, Eaton SM, Bond JP, Neveu W, Moquin D, Noubade R, Briso EM, Charland C, Leonard WJ, Ciliberto G, et al. The induction of antibody production by IL-6 is indirectly mediated by IL-21 produced by CD4+ T cells. J Exp Med. 2009; 206:69–78. [PubMed: 19139170]

Dienz O, Rud JG, Eaton SM, Lanthier PA, Burg E, Drew A, Bunn J, Suratt BT, Haynes L, Rincon M. Essential role of IL-6 in protection against H1N1 influenza virus by promoting neutrophil survival in the lung. Mucosal Immunol. 2012; 5:258–266. [PubMed: 22294047]

Farley N, Pedraza-Alva G, Serrano-Gomez D, Nagaleekar V, Aronshtam A, Krahl T, Thornton T, Rincon M. p38 mitogen-activated protein kinase mediates the Fas-induced mitochondrial death pathway in CD8+ T cells. Mol Cell Biol. 2006; 26:2118–2129. [PubMed: 16507991]

Frauwirth KA, Riley JL, Harris MH, Parry RV, Rathmell JC, Plas DR, Elstrom RL, June CH, Thompson CB. The CD28 signaling pathway regulates glucose metabolism. Immunity. 2002; 16:769–777. [PubMed: 12121659]

Gomperts BD. Exocytosis: the role of Ca2+, GTP and ATP as regulators and modulators in the rat mast cell model. Journal of experimental pathology. 1990; 71:423–431. [PubMed: 2196917]

Hatle K, Gummadidala P, Navasa N, Bernardo E, Dodge J, Silverstrim B, Fortner K, Burg E, Suratt BT, Hammer J, et al. MCJ/DnaJC15, an endogenous mitochondrial repressor of the respiratory chain that controls metabolic alterations. Mol Cell Biol. 2013; 33:2302–2314. [PubMed: 23530063]

Hatle KM, Neveu W, Dienz O, Rymarchyk S, Barrantes R, Hale S, Farley N, Lounsbury KM, Bond JP, Taatjes D, Rincon M. Methylation-controlled J protein promotes c-Jun degradation to prevent ABCB1 transporter expression. Mol Cell Biol. 2007a; 27:2952–2966. [PubMed: 17283040]

Hatle KM, Neveu W, Dienz O, Rymarchyk S, Barrantes R, Hale S, Farley N, Lounsbury KM, Bond JP, Taatjes D, Rincon M. Methylation-controlled J protein promotes c-Jun degradation to prevent ABCB1 transporter expression. Molecular and cellular biology. 2007b; 27:2952–2966. [PubMed: 17283040]

Hogquist KA, Jameson SC, Heath WR, Howard JL, Bevan MJ, Carbone FR. T cell receptor antagonist peptides induce positive selection. Cell. 1994; 76:17–27. [PubMed: 8287475]

Jameson SC, Masopust D. Diversity in T cell memory: an embarrassment of riches. Immunity. 2009; 31:859–871. [PubMed: 20064446]

Jelley-Gibbs DM, Dibble JP, Brown DM, Strutt TM, McKinstry KK, Swain SL. Persistent depots of influenza antigen fail to induce a cytotoxic CD8 T cell response. J Immunol. 2007; 178:7563–7570. [PubMed: 17548591]

Jena BP. Porosome: the secretory NanoMachine in cells. Methods Mol Biol. 2013; 931:345–365. [PubMed: 23027011]

Jitrapakdee S, Wutthisathapornchai A, Wallace JC, MacDonald MJ. Regulation of insulin secretion: role of mitochondrial signalling. Diabetologia. 2010; 53:1019–1032. [PubMed: 20225132]

John LB, Ward AC. The Ikaros gene family: transcriptional regulators of hematopoiesis and immunity. Mol Immunol. 2011; 48:1272–1278. [PubMed: 21477865]

Kaech SM, Tan JT, Wherry EJ, Konieczny BT, Surh CD, Ahmed R. Selective expression of the interleukin 7 receptor identifies effector CD8 T cells that give rise to long-lived memory cells. Nat Immunol. 2003; 4:1191–1198. [PubMed: 14625547]

Kaech SM, Wherry EJ. Heterogeneity and cell-fate decisions in effector and memory CD8+ T cell differentiation during viral infection. Immunity. 2007; 27:393–405. [PubMed: 17892848]

Krauss S, Brand MD, Buttgereit F. Signaling takes a breath--new quantitative perspectives on bioenergetics and signal transduction. Immunity. 2001; 15:497–502. [PubMed: 11672532]

La Gruta NL, Turner SJ. T cell mediated immunity to influenza: mechanisms of viral control. Trends Immunol. 2014; 35:396–402. [PubMed: 25043801]

MacDonald HR. Energy metabolism and T-cell-mediated cytolysis. II. Selective inhibition of cytolysis by 2-deoxy-D-glucose. J Exp Med. 1977; 146:710–719. [PubMed: 302305]

MacDonald HR, Koch CJ. Energy metabolism and T-cell-mediated cytolysis. I. Synergism between inhibitors of respiration and glycolysis. J Exp Med. 1977; 146:698–709. [PubMed: 302304]

Macintyre AN, Finlay D, Preston G, Sinclair LV, Waugh CM, Tamas P, Feijoo C, Okkenhaug K, Cantrell DA. Protein kinase B controls transcriptional programs that direct cytotoxic T cell fate but is dispensable for T cell metabolism. Immunity. 2011; 34:224–236. [PubMed: 21295499]

McElroy DS, Badstibner AM, D'Orazio SE. Use of the CD107 mobilization assay reveals that cytotoxic T lymphocytes with novel MHC-Ib restriction are activated during Listeria monocytogenes infection. J Immunol Methods. 2007; 328:45–52. [PubMed: 17900608]

Monteleone M, Stow JL, Schroder K. Mechanisms of unconventional secretion of IL-1 family cytokines. Cytokine. 2015; 74:213–218. [PubMed: 25922276]

Moreno-Lastres D, Fontanesi F, Garcia-Consuegra I, Martin MA, Arenas J, Barrientos A, Ugalde C. Mitochondrial complex I plays an essential role in human respirasome assembly. Cell Metab. 2012; 15:324–335. [PubMed: 22342700]

Morlino G, Barreiro O, Baixauli F, Robles-Valero J, Gonzalez-Granado JM, Villa-Bellosta R, Cuenca J, Sanchez-Sorzano CO, Veiga E, Martin-Cofreces NB, Sanchez-Madrid F. Miro-1 links mitochondria and microtubule Dynein motors to control lymphocyte migration and polarity. Mol Cell Biol. 2014; 34:1412–1426. [PubMed: 24492963]

Navasa N, Martin I, Iglesias-Pedraz JM, Beraza N, Atondo E, Izadi H, Ayaz F, Fernandez-Alvarez S, Hatle K, Som A, et al. Regulation of oxidative stress by methylation-controlled J protein controls macrophage responses to inflammatory insults. J Infect Dis. 2015a; 211:135–145. [PubMed: 25028693]

Navasa N, Martin-Ruiz I, Atondo E, Sutherland JD, Angel Pascual-Itoiz M, Carreras-Gonzalez A, Izadi H, Tomas-Cortazar J, Ayaz F, Martin-Martin N, et al. Ikaros mediates the DNA methylation-independent silencing of MCJ/DNAJC15 gene expression in macrophages. Scientific reports. 2015b; 5:14692. [PubMed: 26419808]

O'Brien S, Thomas RM, Wertheim GB, Zhang F, Shen H, Wells AD. Ikaros imposes a barrier to CD8+ T cell differentiation by restricting autocrine IL-2 production. J Immunol. 2014; 192:5118–5129. [PubMed: 24778448]

O'Sullivan D, van der Windt GJ, Huang SC, Curtis JD, Chang CH, Buck MD, Qiu J, Smith AM, Lam WY, DiPlato LM, et al. Memory CD8(+) T cells use cell-intrinsic lipolysis to support the metabolic programming necessary for development. Immunity. 2014; 41:75–88. [PubMed: 25001241]

Okoye I, Wang L, Pallmer K, Richter K, Ichimura T, Haas R, Crouse J, Choi O, Heathcote D, Lovo E, et al. T cell metabolism. The protein LEM promotes CD8(+) T cell immunity through effects on mitochondrial respiration. Science. 2015; 348:995–1001. [PubMed: 25883318]

Olson JA, McDonald-Hyman C, Jameson SC, Hamilton SE. Effector-like CD8(+) T cells in the memory population mediate potent protective immunity. Immunity. 2013; 38:1250–1260. [PubMed: 23746652]

Pearce EL, Poffenberger MC, Chang CH, Jones RG. Fueling immunity: insights into metabolism and lymphocyte function. Science. 2013; 342:1242454. [PubMed: 24115444]

Pearce EL, Walsh MC, Cejas PJ, Harms GM, Shen H, Wang LS, Jones RG, Choi Y. Enhancing CD8 T-cell memory by modulating fatty acid metabolism. Nature. 2009; 460:103–107. [PubMed: 19494812]

Pene J, Gauchat JF, Lecart S, Drouet E, Guglielmi P, Boulay V, Delwail A, Foster D, Lecron JC, Yssel H. Cutting edge: IL-21 is a switch factor for the production of IgG1 and IgG3 by human B cells. Journal of immunology. 2004; 172:5154–5157.

Powell TJ, Strutt T, Reome J, Hollenbaugh JA, Roberts AD, Woodland DL, Swain SL, Dutton RW. Priming with cold-adapted influenza A does not prevent infection but elicits long-lived protection against supralethal challenge with heterosubtypic virus. J Immunol. 2007; 178:1030–1038. [PubMed: 17202366]

Rao AS, Kim D, Nam H, Jo H, Kim KH, Ban C, Ahn KH. A turn-on two-photon fluorescent probe for ATP and ADP. Chem Commun (Camb). 2012; 48:3206–3208. [PubMed: 22331239]

Rathmell JC, Vander Heiden MG, Harris MH, Frauwirth KA, Thompson CB. In the absence of extrinsic signals, nutrient utilization by lymphocytes is insufficient to maintain either cell size or viability. Mol Cell. 2000; 6:683–692. [PubMed: 11030347]

Salabei JK, Gibb AA, Hill BG. Comprehensive measurement of respiratory activity in permeabilized cells using extracellular flux analysis. Nat Protoc. 2014; 9:421–438. [PubMed: 24457333]

Sallusto F, Geginat J, Lanzavecchia A. Central memory and effector memory T cell subsets: function, generation, and maintenance. Annu Rev Immunol. 2004; 22:745–763. [PubMed: 15032595]

Sarkar S, Kalia V, Haining WN, Konieczny BT, Subramaniam S, Ahmed R. Functional and genomic profiling of effector CD8 T cell subsets with distinct memory fates. J Exp Med. 2008; 205:625–640. [PubMed: 18316415]

Schusdziarra C, Blamowska M, Azem A, Hell K. Methylation-controlled J-protein MCJ acts in the import of proteins into human mitochondria. Hum Mol Genet. 2013; 22:1348–1357. [PubMed: 23263864]

Shridhar V, Bible KC, Staub J, Avula R, Lee YK, Kalli K, Huang H, Hartmann LC, Kaufmann SH, Smith DI. Loss of expression of a new member of the DNAJ protein family confers resistance to chemotherapeutic agents used in the treatment of ovarian cancer. Cancer Res. 2001; 61:4258–4265. [PubMed: 11358853]

Strathdee G, Davies BR, Vass JK, Siddiqui N, Brown R. Cell type-specific methylation of an intronic CpG island controls expression of the MCJ gene. Carcinogenesis. 2004; 25:693–701. [PubMed: 14729589]

Strathdee G, Vass JK, Oien KA, Siddiqui N, Curto-Garcia J, Brown R. Demethylation of the MCJ gene in stage III/IV epithelial ovarian cancer and response to chemotherapy. Gynecol Oncol. 2005; 97:898–903. [PubMed: 15894365]

van der Windt GJ, Everts B, Chang CH, Curtis JD, Freitas TC, Amiel E, Pearce EJ, Pearce EL. Mitochondrial respiratory capacity is a critical regulator of CD8+ T cell memory development. Immunity. 2012; 36:68–78. [PubMed: 22206904]

van der Windt GJ, O'Sullivan D, Everts B, Huang SC-C, Buck MD, Curtis JD, Chang CH, Smith AM, Brandon TA, Faubert B, et al. CD8 memory T cells have a bioenergetic advantage that underlines their rapid recall ability. Proc Natl Acad Sci U S A. 2013 in press.

van der Windt GJ, Pearce EL. Metabolic switching and fuel choice during T-cell differentiation and memory development. Immunol Rev. 2012; 249:27–42. [PubMed: 22889213]

Vukotic M, Oeljeklaus S, Wiese S, Vogtle FN, Meisinger C, Meyer HE, Zieseniss A, Katschinski DM, Jans DC, Jakobs S, et al. Rcf1 mediates cytochrome oxidase assembly and respirasome formation, revealing heterogeneity of the enzyme complex. Cell Metab. 2012; 15:336–347. [PubMed: 22342701]

Wahl DR, Byersdorfer CA, Ferrara JL, Opipari AW Jr, Glick GD. Distinct metabolic programs in activated T cells: opportunities for selective immunomodulation. Immunol Rev. 2012; 249:104–115. [PubMed: 22889218]

Wang R, Dillon CP, Shi LZ, Milasta S, Carter R, Finkelstein D, McCormick LL, Fitzgerald P, Chi H, Munger J, Green DR. The transcription factor Myc controls metabolic reprogramming upon T lymphocyte activation. Immunity. 2011; 35:871–882. [PubMed: 22195744]

Wang R, Green DR. Metabolic reprogramming and metabolic dependency in T cells. Immunol Rev. 2012; 249:14–26. [PubMed: 22889212]

Wiederkehr A, Wollheim CB. Minireview: implication of mitochondria in insulin secretion and action. Endocrinology. 2006; 147:2643–2649. [PubMed: 16556766]

Yang DD, Conze D, Whitmarsh AJ, Barret T, Davis RJ, Rincón M, Flavell RA. Differentiation of $CD4^+$ T cells to Th1 cells requires MAP kinase JNK2. Immunity. 1998; 9:575–585. [PubMed: 9806643]

Yang R, Lirussi D, Thornton TM, Jelley-Gibbs DM, Diehl SA, Case LK, Madesh M, Taatjes DJ, Teuscher C, Haynes L, Rincon M. Mitochondrial Ca(2)(+) and membrane potential, an alternative pathway for Interleukin 6 to regulate CD4 cell effector function. eLife. 2015; 4

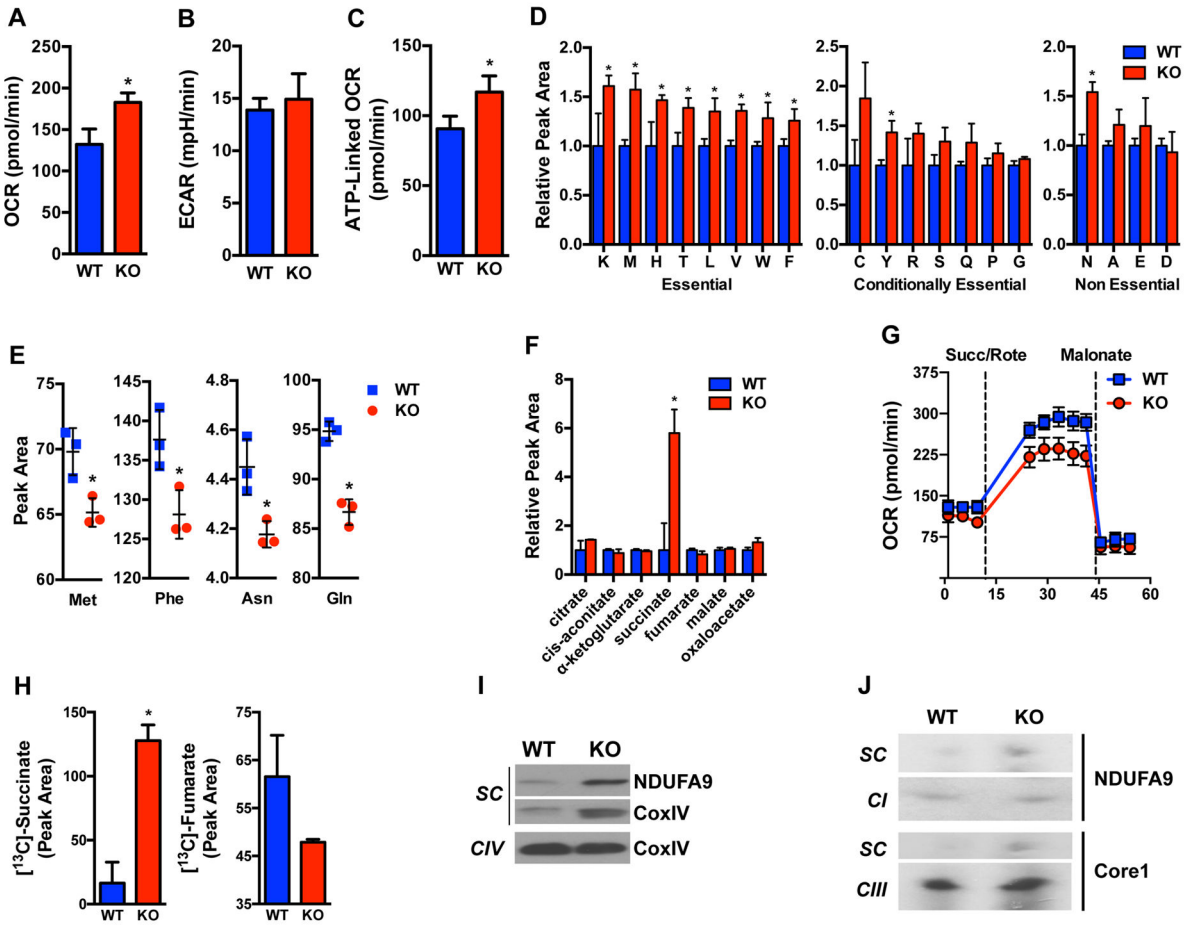

Figure 1. MCJ serves to restrain mitochondrial respiration in naïve CD8 T cells

(**A**) Baseline oxygen consumption rate (OCR) (n= 4), (**B**) Extracellular acidification rate (ECAR) (n=5), and (**C**) OCR linked to mitochondrial ATP production (meaning baseline OCR minus OCR in the presence of oligomycin) of CD8 cells freshly isolated from WT and MCJ KO mice were determined using the Seahorse MitoStress assay (**A**, **C**) or Glycolysis Stress assay (**B**) and a Seahorse Bioscience XF24 analyzer. (**D** and **F**) CD8 cells were purified from WT and MCJ KO mice (n=3 mice) and their metabolic profiles were determined by UPLC-MS. Relative amounts of (**D**) amino acids and (**F**) metabolites of the tricarboxylic acid (TCA) cycle are shown. (**E**) Equal numbers of CD8 cells freshly isolated from WT and MCJ KO mice (n=3) were incubated with culture medium for 16 h, and the metabolic profile of the culture supernatants was determined as in (**D** and **F**). (**G**) Complex II linked mitochondrial respiration in permeabilized CD8 cells was determined using a Seahorse Bioscience XF24 analyzer. Freshly isolated WT and MCJ KO CD8 cells were permeabilized using XF Plasma Membrane Permeabilizer and OCR was determined at baseline, in the presence of succinate with rotenone (Succ/Rote) and malonate. (**H**) CD8 cells were purified from WT and MCJ KO mice (n=3), cultured in the presence of ^{13}C and ^{15}N labeled amino acids for 5 min or 5 h, and metabolic flux was determined by UPLC-MS analysis. Levels of ^{13}C-succinate and ^{13}C-fumarate are shown. (**I**, **J**) Mitochondrial extracts from CD8 cells isolated from WT and MCJ KO mice were solubilized with

digitonin and resolved by blue native electrophoresis. (**I**) Bands corresponding to mitochondrial supercomplexes (*SC*) were excised, resolved by SDS-PAGE, and examined by Western blot analysis for NDUFA9 (Complex I) and CoxIV (Complex IV). The band corresponding to monomeric Complex IV (*CIV*) was also excised and examined as control. (**J**) Proteins separated by BNE were transferred to PVDF membrane and examined by Western blot analysis for subunits of Complexes I (NDUFA9) and III (Core1). Bands corresponding to supercomplexes (SC) and monomeric Complexes I (*CI*) and III (*CIII*) regions of the Western blot are shown. *, denotes $p < 0.05$ as determined by unpaired *t* test ($n \geq 3$).

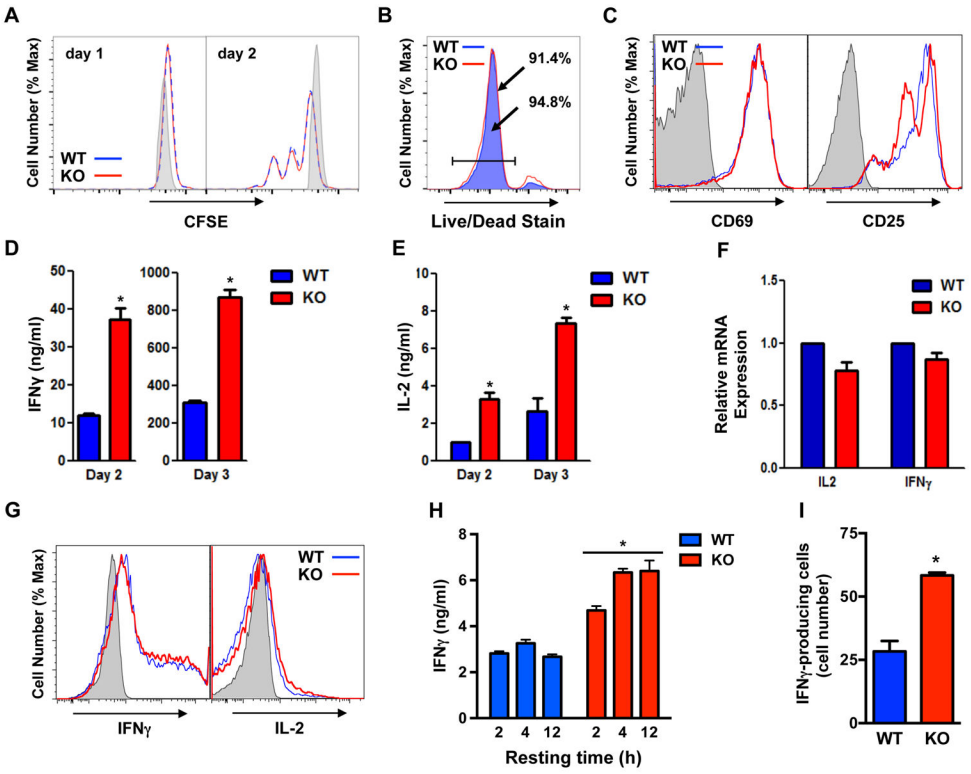

Figure 2. MCJ deficiency does not affect effector CD8 cell proliferation but increases the secretion of cytokines

(**A**) Proliferation of WT (blue) and MCJ KO (red) CD8 cells after activation with anti-CD3 and anti-CD28 Abs for one or two days was determined by CFSE staining and flow cytometry analysis. Gray histograms show the CFSE profiles for cells immediately after staining. (**B**) Cell survival of WT (blue) and MCJ KO (red) CD8 cells after 2 days of activation with anti-CD3 and anti-CD28 Abs was determined by Live/Dead staining and flow cytometry analysis. (**C**) Cell surface expression of CD69 and CD25 on WT (blue) and MCJ KO (red) CD8 cells activated for 2 d as described (A) was determined by flow cytometry analysis. Shaded histograms represent unstained cells. (**D–E**) Culture supernatants of WT and MCJ KO CD8 cells activated for 2 or 3 days were examined for (**D**) IFNγ and (**E**) IL-2 by ELISA (n=3). (**F**) Relative mRNA levels for IL-2 and IFNγ in WT and MCJ KO CD8 cells activated for 2 d as determined by qRT-PCR. (**G**) Intracellular levels of IFNγ and IL-2 in WT (blue) and MCJ KO (red) CD8 cells activated for 2 days were determined by intracellular staining and flow cytometry analysis. Shaded histograms show unstained cells. (**H**) WT and MCJ KO CD8 cells were activated for 2 d, washed, and replated at equal numbers in medium alone for the indicated times. Levels of IFNγ in the culture supernatants were determined by ELISA. (**I**) WT and MJC KO CD8 cells were activated for 2 days, and the number of IFNγ-producing cells was determined by ELISpot assay (n=3). *, denotes $p < 0.05$ as determined by unpaired *t* test.

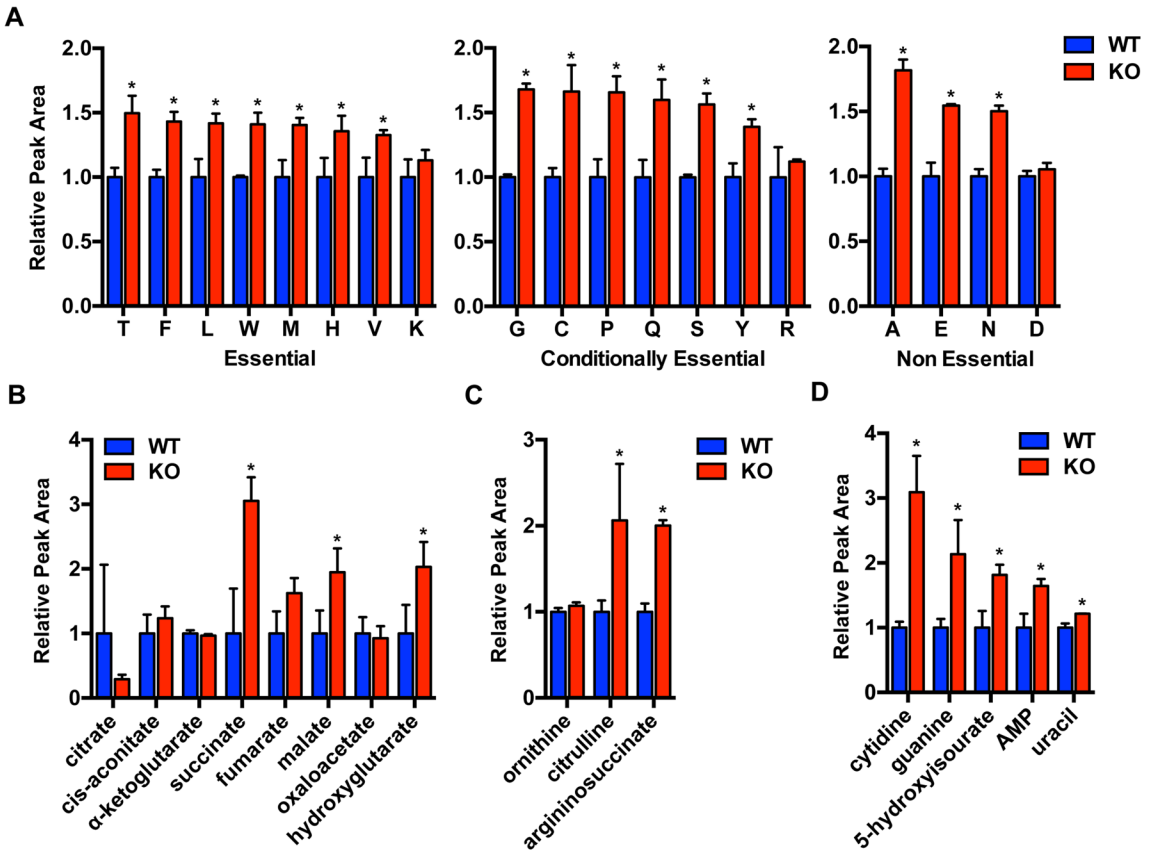

Figure 3. MCJ deficiency enhances mitochondrial metabolism in effector CD8 cells

(**A**–**D**) CD8 cells isolated from WT and MCJ KO mice (n=3) were activated for 2 days, and their metabolic profile was determined by UPLC-MS (2×10^6 cells/ml). Relative levels of (**A**) amino acids and (**B**) metabolites of the TCA cycle (**C**), urea cycle (**D**) and nucleotide pathways are shown. *, denotes $p < 0.05$ as determined by unpaired *t* test.

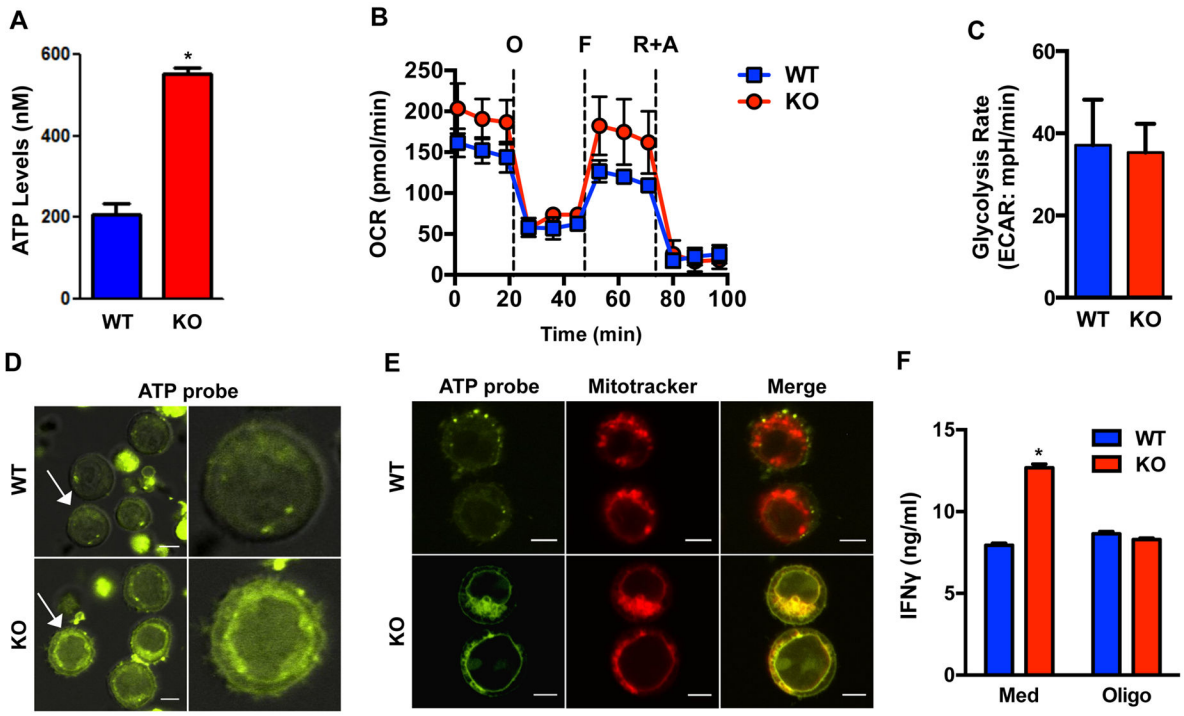

Figure 4. Increased oxidative phosphorylation in MCJ-deficient effector CD8 cells facilitates IFNγ secretion

(**A**) ATP levels in WT and MCJ KO CD8 cells activated for 2 days and rested for 4 h. (**B**) Oxygen consumption rate (OCR) of WT and MCJ KO CD8 cells (n=4) activated for 2 d and rested for 12 h was determined in the presence of medium, oligomycin (O), FCCP (F), and rotenone and antimycim (R+A) using the Seahorse MitoStress assay. (**C**) Relative glycolysis rate determined by ECAR in activated WT and MCJ KO CD8 cells (n=10) after addition of glucose (10 mM) using the Seahorse Glycolytic assay. (**D**) WT and MCJ KO CD8 cells were activated for 2 d, live stained for 5 min with the ATP-probe (green), washed, and visualized by confocal microscopy. Scale bar represents 10 nm. Right panels show a magnification of the cells indicated by the white arrows. (**E**) WT and MCJ KO CD8 cells were activated, stained with Mitotracker (red) followed by staining for 5 min (live staining) with the ATP probe (green), washed, and visualized by confocal microscopy. Single staining and costaining of mitotracker and ATP probe are shown. Scale bar represents 10 nm. (**F**) WT and MCJ KO CD8 cells were activated for 2 days, incubated with oligomycin during the last 4 h of activation, washed, counted, and replated in medium alone for 4 h. IFNγ levels in the supernatants were determined by ELISA. *, denotes $p < 0.05$ as determined by unpaired *t* test.

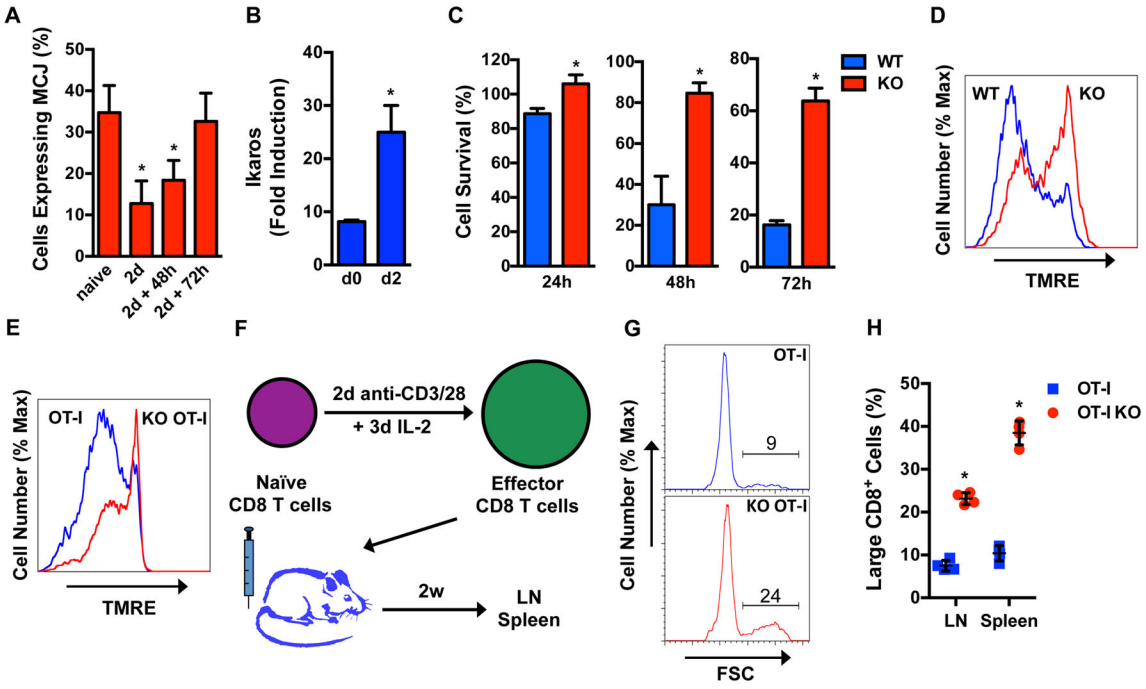

Figure 5. MCJ deficiency sustains the metabolic activity of effector CD8 cells during the contraction phase

(**A**) Frequency of β-galactosidase positive CD8 cells from MCJ KO mice either freshly isolated (naïve), activated for 2 days (2d), or activated for 2 days and rested in medium for 48 h (2d + 48h) or 72 h (2d + 72h) as determined by flow cytometry analysis. (**B**) CD8 cells from WT and MCJ KO mice were analyzed for Ikaros binding to the MCJ promoter by chromatin immunoprecipitation (ChIP) assay. Cells were freshly isolated (d0) or activated with anti-CD3/CD28 Abs for 2 days (d2). Bars indicate the fold increase over rabbit IgG immunoprecipitates relative to input. (**C**) WT and MCJ KO CD8 cells were activated for 2 d, washed, and equal numbers of cells were incubated in medium without stimulation or cytokines for 24, 48, and 72 h. The number of live cells recovered relative to the initial number is shown. (**D**) WT (blue) and MCJ KO (red) CD8 cells were activated for 2 d, rested in medium without stimulation for 48 h, and MMP was examined by staining with TMRE and flow cytometry analysis. (**E**) MMP was examined by staining with TMRE and flow cytometry analysis in freshly isolated OT-I (blue) and MCJ KO OT-I (red) CD8 cells. (**F**, **G**, **H**) OT-I (CD90.1$^+$) and MCJ KO OT-I (CD90.1$^+$ CD90.2$^+$) CD8 cells were activated with anti-CD3/CD28 Abs for 2 d, and then expanded in the presence of IL-2 for 3 d. A mix of equal numbers of WT and MCJ KO cells were adoptively transferred into WT (C57BL/6) (CD90.2$^+$) recipient mice (n=4). Lymph nodes (LN) and spleen were harvested after 2 weeks (**F**). Blastic stage of cells was defined by high forward scatter (FSC) examined by flow cytometry in gated OT-I (CD90.1$^+$) and MCJ KO OT-I (CD90.1$^+$ CD90.2$^+$) CD8 cells (**G**). The frequency of OT-I and MCJ KO OT-I CD8 cells with high forward scatter within each recipient mouse (n=4) was determined (**H**). *, denotes $p<0.05$ as determined by unpaired *t* test.

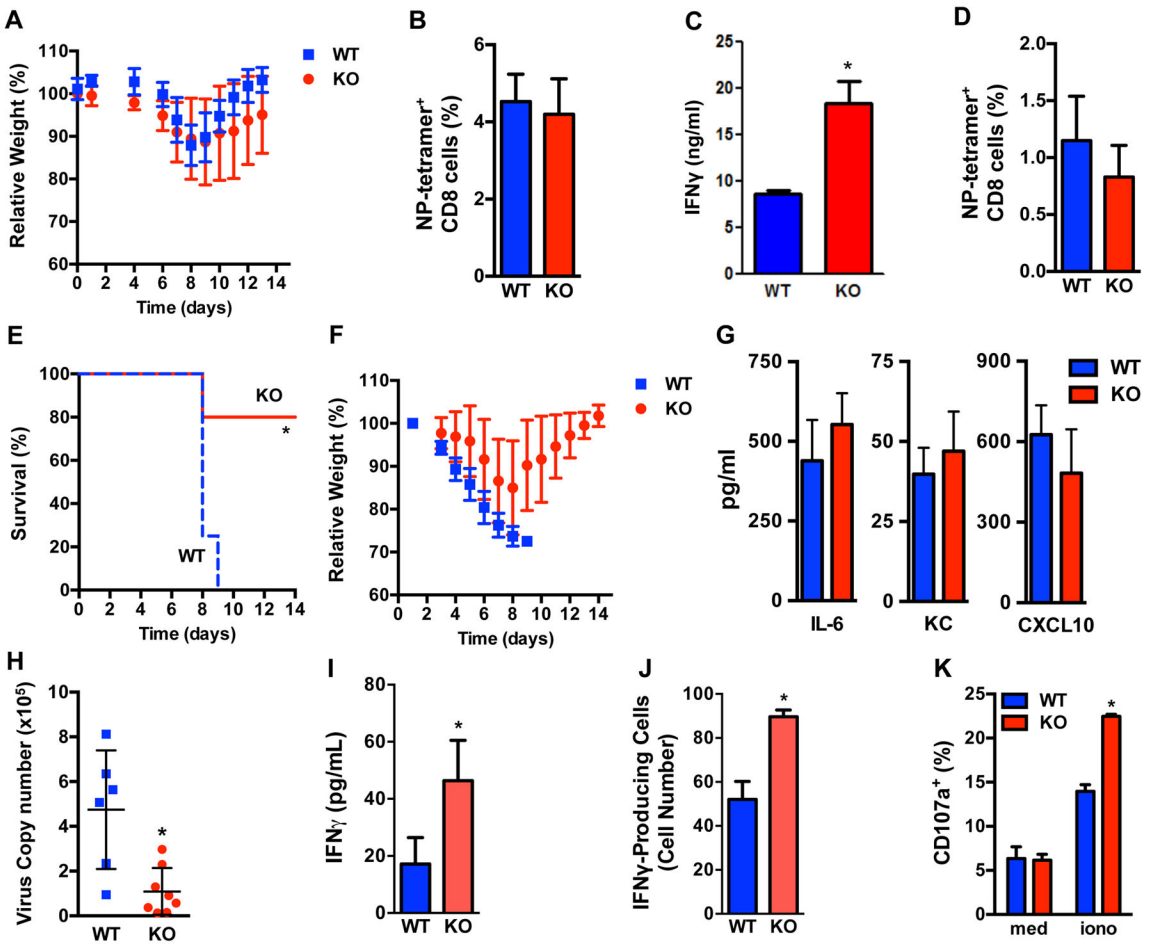

Figure 6. Loss of MCJ confers viral protective activity to memory CD8 cells

(**A**) WT and MCJ KO mice (n=5) were infected with a sublethal dose of PR8 influenza virus (primary infection). Percent weight loss over time after infection is shown. (**B** and **C**) CD8 cells were isolated from the spleen and draining mediastinal lymph node (MLN) of WT and MCJ KO mice (n=4) 2 weeks after a primary infection with influenza PR8 virus. (**B**) The percentage of NP-tetramer positive cells in CD8 cells in the spleen was determined by flow cytometry analysis. (**C**) CD8 cells from the spleen and MLN were cultured *ex vivo* in medium, and IFNγ secreted into the supernatant was determined by ELISA. (**D**) NP-tetramer positive CD8 cells from spleen/MLN of WT and MCJ KO mice (n=5) five weeks after infection with a sublethal dose of PR8 influenza virus as described in (A). (**E, F**) WT and MCJ KO mice were infected with a sublethal dose of PR8 influenza virus. CD8 cells were isolated from those mice 5 weeks after infection and adoptively transferred into naïve WT recipient mice (n=5). Recipient mice were then infected with a lethal dose of PR8 virus. Survival (**E**) and weight loss (**F**) of the recipient mice after lethal infection are shown. (**G** – **K**) Recipient WT mice (n=4) that received CD8 cells from either infected WT and MCJ KO mice as described in (E) were infected with a lethal dose of PR8 virus. Mice were sacrificed 6 days after the lethal infection. (**G**) Cytokine levels in BALF as determined by Luminex assay. (**H**) PR8 virus titer in lung as determined by real time RT-PCR. (**I**) WT and MCJ KO CD8 cells isolated from the draining mediastinal LN from the lethally infected mice were

cultured *ex vivo* in medium alone and IFNγ secreted into the culture supernatant was determined by ELISA. (**J**) WT and MCJ KO CD8 cells from the lung were analyzed for IFNγ secretion by ELISpot assay. (**K**) WT and MCJ KO CD8 cells from MLN were analyzed by CD107a mobilization assay, a measure of degranulation and cytotoxic capacity, by examining CD107a expression on the cell surface by flow cytometry analysis. Percentage of CD107a-positive CD8 cells is shown. For the Kaplan-Meier survival curve, * denotes $p<0.05$ by log-rank test. For all others, * denotes $p<0.05$ as determined by unpaired *t* test.